Fig. 2 Time course of platelet counts during the first 5 days of ICU stay in patients with sepsis, showing patients with a subsequent decrease in platelet count (solid line) vs patients without a subsequent decrease in platelet count (dotted line). A subsequent decrease in platelet count was defined as a decrease of 30% or more within 5 days of ICU admission. Day 1, the day of ICU admission. Data are expressed as mean and 95% CIs; $*P < .05$.

3.2. Relationships of hemostatic biomarkers with a subsequent decrease in platelet count in patients with sepsis

We evaluated coagulation and fibrinolytic markers on the day of ICU admission and examined their relationship with a subsequent decrease in platelet count. There were significant differences between patients with and patients without a subsequent decrease in platelet count in PT-INR (median, 1.33 vs 1.17; $P = .048$), fibrinogen (322 vs 526, $P = .0014$), TAT (13.8 vs 7.2, $P < .0001$), AT (51.1 vs 62.7, $P = .0099$), PC (35.1 vs 64.2, $P = .0002$), plasminogen (50.7 vs 85.3, $P = .0007$), and α_2-PI (56.3 vs 83.9, $P = .0001$) (Table 3). There were no significant differences between the 2 groups in APTT, FDP, or PIC.

3.3. Ability of hemostatic biomarkers to predict a subsequent decrease in platelet count in patients with sepsis

We conducted ROC curve analysis to evaluate the ability of hemostatic biomarkers to predict a subsequent decrease in

platelet count. The AUC and best calculated cutoff values for prediction of a subsequent decrease in platelet count are shown in Table 4. The AUC for prediction of a subsequent decrease in platelet count was high for α_2-PI (0.885), PC (0.869), plasminogen (0.846), and TAT (0.846), compared with PT-INR (0.639) and fibrinogen (0.666). Interestingly, the ability to predict a subsequent decrease in platelet count was significantly higher for PC (AUC, 0.869; 95% confidence interval [CI], 0.699-0.951; $P = .0098$) and α_2-PI (AUC, 0.885; 95% CI, 0.714-0.959; $P = .029$), in pairwise comparison with PT-INR (AUC, 0.639; 95% CI, 0.432-0.799) (Fig. 3).

4. Discussion

In this retrospective study, we evaluated the usefulness of a single measurement of coagulation and fibrinolytic biomarkers on the day of ICU admission, for providing simple and prompt assessment for progression of coagulopathy in patients with sepsis. Our results show that decreased PC and α_2-PI activity were strong predictors of a subsequent decrease in platelet count, which was considered as an indicator of overt coagulopathy in sepsis.

Currently, there are no widely accepted diagnostic criteria for early stage of septic coagulopathy. Intervention to coagulopathy in initial phase might be one of the key factors in improving outcomes in patients with sepsis. Several researchers have recently established diagnostic scoring systems for the acute phase of septic coagulopathy [21-23], but these systems depend partly on changes in biomarker levels from baseline, which take at least 2 days to identify. Our results suggest that the progression of septic coagulopathy could be detected by a single measurement of PC and α_2-PI, which would help to develop early diagnostic criteria for septic coagulopathy.

Previous studies have evaluated the prognostic values of hemostatic biomarkers in patients with sepsis, but the reported results have been inconsistent [1,9,21,24]. These conflicting results may be partly caused by the multiple

Table 3	Comparison of coagulation and fibrinolytic markers on the day of ICU admission			
	Reference range	Subsequent decrease in platelet count (n = 42)	No subsequent decrease in platelet count (n = 33)	P
Platelet count ($\times 10^3/\mu L$)	130-369	181 (123-245)	197 (162-234)	.52
PT-INR	0.9-1.2	1.33 (1.14-1.53)	1.17 (1.11-1.34)	.048
APTT (s)	23.1-36.3	44.2 (32.9-59.3)	40.6 (36.1-48.3)	.71
Fibrinogen (mg/dL)	129-271	322 (212-493)	526 (380-649)	.0014
FDP ($\mu g/mL$)	0-5.0	20.4 (12.3-30.5)	16.8 (11.2-24.3)	.21
TAT (ng/mL)	<2.4	13.8 (9.9-22.1)	7.2 (5.4-9.3)	<.0001
PIC ($\mu g/mL$)	<0.9	0.9 (0.7-1.9)	1.4 (0.8-1.8)	.19
AT (%)	88-116	51.1 (36.9-62.5)	62.7 (47.8-74.1)	.0099
PC (%)	67-129	35.1 (28.1-55.8)	64.2 (56.5-79.8)	.0002
Plasminogen (%)	85-120	50.7 (40.4-68.3)	85.3 (73.9-91.9)	.0007
α_2-PI (%)	83-115	56.5 (48.3-67.6)	83.9 (75.2-94.7)	.0001

Table 4 ROC curve analyses showing AUCs for prediction of a subsequent decrease in platelet count and cutoff values maximizing the sum of sensitivity and specificity

	AUC	P	Cutoff value	Sensitivity	Specificity
Platelet count	0.544	.79	$157 \times 10^3/\mu L$	0.36	0.82
PT-INR	0.639	.012	1.37	0.48	0.79
APTT	0.526	.26	48.9 s	0.45	0.76
Fibrinogen	0.666	.0019	462 mg/dL	0.71	0.66
FDP	0.587	.045	29.4 μg/mL	0.33	0.88
TAT	0.846	<.0001	13 ng/mL	0.59	1.0
PIC	0.399	.57	2.7 μg/mL	0.24	0.88
AT	0.734	.0071	55.8%	0.67	0.66
PC	0.869	<.0001	41.4%	0.67	0.94
Plasminogen	0.846	.0012	72.8%	0.91	0.77
α_2-PI	0.885	<.0001	73.3%	0.92	0.75

interactive systemic factors that are involved in the pathogenesis of organ failure and the risk of mortality, although cytokine-induced coagulopathy is considered to play a major role in the process [25]. In addition, not only the development but also subsequent progression or persistence of coagulopathy are associated with poor prognosis in patients with sepsis [9,21]. We therefore focused on the progression of coagulopathy as an outcome in patients in the acute phase of sepsis.

Because there are no established criteria for assessing the progression of septic coagulopathy, we used decreasing in platelet count as a marker of disease progression. Most diagnostic criteria for DIC, including the ISTH criteria, primarily use global coagulation tests such as PT, platelet count, fibrinogen, and FDP for scoring. These markers change differently over time as coagulopathy progresses. Production of FDP may be suppressed in severe coagulopathy because of a massive increase in PAI-1 level, and the fibrinogen level tends to increase with acute-phase behavior in septic patients [26]. In addition, appropriate thresholds for the diagnosis of septic coagulopathy have not been determined. Although coagulopathy is universal in severe sepsis, only about 30% of patients in a large multicenter trial met the ISTH criteria for overt DIC [4]. The current diagnostic criteria are not useful for the evaluation of disease progression in septic patients with coagulopathy.

Thrombocytopenia is common in critically ill patients with an incidence of 40% to 50% [27], and a 30% decrease in platelet count during ICU admission has been shown to be associated with increased mortality [28]. Thrombocytopenia can be a result of many causes such as blood loss, hemodilution, thrombotic microangiopathy, and immune and drug-induced thrombocytopenia. However, septic coagulopathy is the most common underlying cause [26]. Although a diagnosis of DIC must be supported by multiple laboratory tests and other causes of thrombocytopenia should be ruled out, thrombocytopenia is a relevant marker of DIC [5]. In addition, it has been clinically recognized that thrombocytopenia may be a warning sign of severe sepsis and that the decrease in platelet count is related to the

severity of sepsis [29]. In our study, a significant decrease in platelet count after ICU admission was associated with disease severity, the incidence of organ dysfunction, and the 28-day mortality rate (Tables 1 and 2).

In our study, AT, PC, plasminogen, α_2-PI activity, and TAT on the day of ICU admission had high predictive values for a subsequent decrease in platelet count in patients with sepsis. In sepsis, physiological anticoagulation mechanisms such as the AT and PC systems are impaired because of increased consumption, impaired synthesis, extravasation from vessels, and degradation by several proteolytic enzymes such as neutrophil elastase [30,31]. We found that AT and PC activity were significantly decreased in patients with a subsequent decrease in platelet count compared with patients without a subsequent decrease in platelet count, which may have been caused by increased consumption. However, mild to moderately decreased AT and PC activity were also observed in patients without a subsequent decrease in platelet count (Table 1). Asakura et al [32] reported that AT and PC activity were related to the plasma albumin level and that decreased AT and PC activity were observed in septic patients without DIC. The mechanisms of decreased AT and PC activity in patients without a subsequent decrease in platelet count may include impaired synthesis, or degradation associated with inflammation, rather than consumption coagulopathy.

We found that PC was a stronger predictor of a subsequent decrease in platelet count than AT, which is somewhat inconsistent with the results of previous studies. Several investigators have reported that AT had a higher [33] or comparable [21] association with poor prognosis, compared with PC. However, Nilsson et al [34] showed that PC had a higher correlation with the results of global clotting tests than AT. Protein C has anticoagulant and fibrinolytic properties with neutralization of PAI-1 [35], whereas AT is an anticoagulant that mainly inhibits thrombin and other procoagulant factors.

Measurement of fibrinolytic markers showed that plasminogen and α_2-PI activity were decreased in patients with a subsequent decrease in platelet count and were near the lower
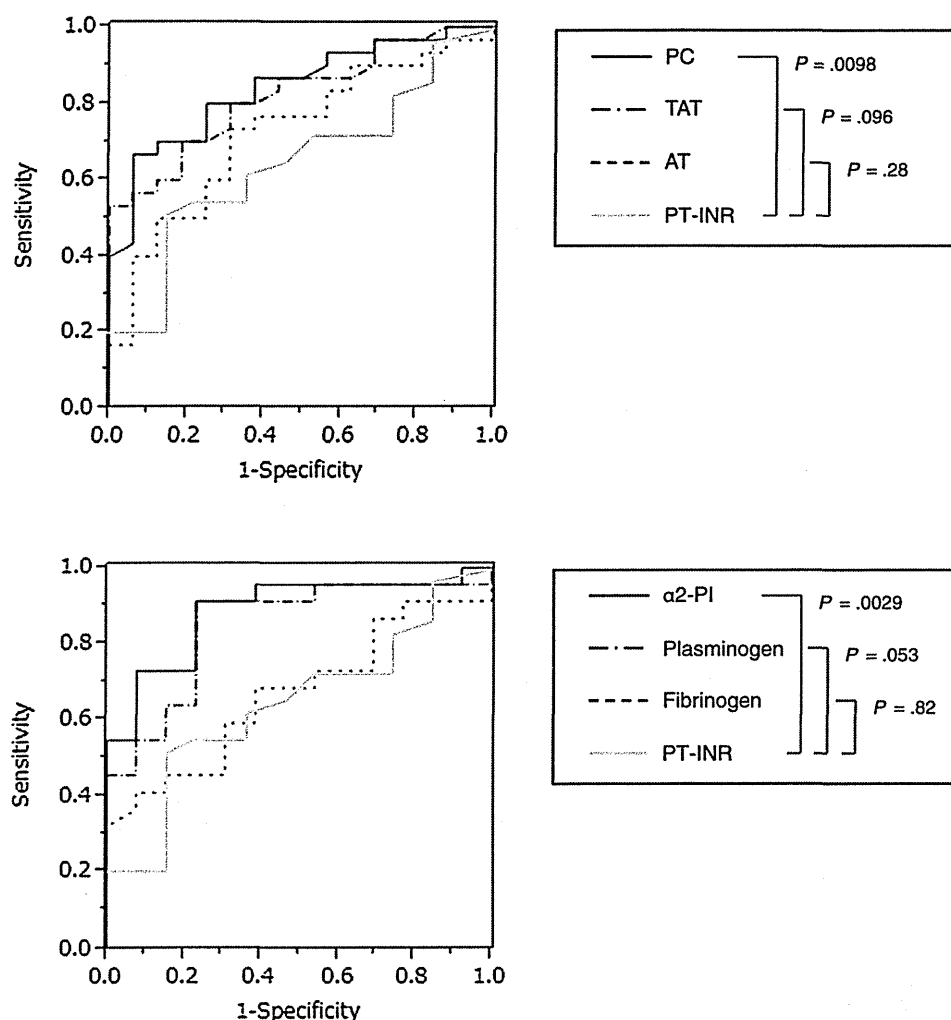
Fig. 3   Pairwise comparisons of ROC curves of biomarkers that significantly predicted a subsequent decrease in platelet count (comparison with the ROC curve of PT-INR).

limit of the reference range in patients without a subsequent decrease in platelet count. These results are consistent with those of previous study, in which only half of the 1690 patients with severe sepsis were shown to have decreased plasminogen and α_2-PI activity, although more than 80% had abnormal AT and PC activity [1]. It is known that the plasminogen activator–plasmin system is markedly depressed by PAI-1 in patients with sepsis [24]. In addition, interleukin-6 induces up-regulation of plasminogen promoter activity [36], and production of plasminogen is increased as an acute-phase protein during sepsis [37]. However, the tissue plasminogen activator level is increased in sepsis [9], and the tissue plasminogen activator/PAI-1 ratio increases with increasing severity of sepsis [33], which may explain why the levels of fibrinolytic markers were decreased under the countered increase of PAI-1.

The present study has some limitations. This was a retrospective observational study that did not promote deviation from routine clinical practices at our institution. Interventions such as treatment of DIC and blood transfusion may have influenced the levels of coagulation and fibrinolytic biomarkers and their relationships with changes in platelet count. Because our study was conducted in a single center, the relatively small size of the study population is also a limitation. A large, prospective study would be useful to validate our results.

In conclusion, decreased PC and α_2-PI activity on the day of ICU admission were strongly associated with a subsequent decrease in platelet count in patients with sepsis. A single measurement of these biomarkers may help to predict progression of septic coagulopathy and guide the decision-making process for early intervention.

Acknowledgments

References

[1] Kinasewitz GT, Yan SB, Basson B, et al. Universal changes in biomarkers of coagulation and inflammation occur in patients with severe sepsis, regardless of causative micro-organism [ISRCTN74215569]. Crit Care 2004;8:R82-0.

[2] Levi M, Ten Cate H. Disseminated intravascular coagulation. N Engl J Med 1999;341:586-92.

[3] Fourrier F, Chopin C, Goudemand J, et al. Septic shock, multiple organ failure, and disseminated intravascular coagulation. Compared patterns of antithrombin III, protein C, and protein S deficiencies. Chest 1992;101:816-23.

[4] Dhainaut JF, Yan SB, Joyce DE, et al. Treatment effects of drotrecogin alfa (activated) in patients with severe sepsis with or without overt disseminated intravascular coagulation. J Thromb Haemost 2004;2: 1924-33.

[5] Ten Cate H. Trombocytopenia: one of the markers of disseminated intravascular coagulation. Pathophysiol Haemost Thromb 2003;33: 413-6.

[6] Wada H, Wakita Y, Nakase T, et al. Outcome of disseminated intravascular coagulation in relation to the score when treatment was begun. Mie DIC Study Group. Thromb Haemost 1995;74: 848-52.

[7] Taylor Jr FB, Toh CH, Hoots WK, et al. Towards definition, clinical and laboratory criteria, and a scoring system for disseminated intravascular coagulation. Thromb Haemost 2001;86: 1327-30.

[8] Oh D, Jang MJ, Lee SJ, et al. Evaluation of modified non-overt DIC criteria on the prediction of poor outcome in patients with sepsis. Thromb Res 2010;126:18-23.

[9] Lorente JA, Garcia-Frade LJ, Landin L, et al. Time course of hemostatic abnormalities in sepsis and its relation to outcome. Chest 1993;103:1536-42.

[10] Wada H, Sakuragawa N, Mori Y, et al. Hemostatic molecular markers before the onset of disseminated intravascular coagulation. Am J Hematol 1999;60:273-8.

[11] Levi M, Opal SM. Coagulation abnormalities in critically ill patients. Crit Care 2006;10:222.

[12] Brun-Buisson C, Doyon F, Carlet J, et al. Incidence, risk factors, and outcome of severe sepsis and septic shock in adults. A multicenter prospective study in intensive care units. French ICU Group for Severe Sepsis. JAMA 1995;274:968-74.

[13] Bone RC, Balk RA, Cerra FB, et al. Definitions for sepsis and organ failure and guidelines for the use of innovative therapies in sepsis. The ACCP/SCCM Consensus Conference Committee. American College of Chest Physicians/Society of Critical Care Medicine. Chest 1992;101:1644-55.

[14] Dellinger RP, Levy MM, Carlet JM, et al. Surviving Sepsis Campaign: international guidelines for management of severe sepsis and septic shock: 2008. Crit Care Med 2008;36:296-327.

[15] Ohno H, Kosaki G, Kambayashi J, et al. FOY: [ethyl P-(6-guanidinohexanoyloxy) benzoate] methanesulfonate as a serine proteinase inhibitor. I. Inhibition of thrombin and factor Xa in vitro. Thromb Res 1980;19:579-88.

[16] Nishiyama T, Matsukawa T, Hanaoka K. Is protease inhibitor a choice for the treatment of pre- or mild disseminated intravascular coagulation? Crit Care Med 2000;28:1419-22.

[17] Knaus WA, Draper EA, Wagner DP, et al. APACHE II: a severity of disease classification system. Crit Care Med 1985;13:818-29.

[18] Le Gall JR, Lemeshow S, Saulnier F. A new Simplified Acute Physiology Score (SAPS II) based on a European/North American multicenter study. JAMA 1993;270:2957-63.

[19] Vincent JL, Moreno R, Takala J, et al. The SOFA (Sepsis-related Organ Failure Assessment) score to describe organ dysfunction/failure. On behalf of the Working Group on Sepsis-Related Problems of the European Society of Intensive Care Medicine. Intensive Care Med 1996;22:707-10.

[20] National Heart L, Blood Institute Acute Respiratory Distress Syndrome Clinical Trials NWiedemann HP, et al. Comparison of two fluid-management strategies in acute lung injury. N Engl J Med 2006;354:2564-75.

[21] Dhainaut JF, Shorr AF, Macias WL, et al. Dynamic evolution of coagulopathy in the first day of severe sepsis: relationship with mortality and organ failure. Crit Care Med 2005;33:341-8.

[22] Gando S, Iba T, Eguchi Y, et al. A multicenter, prospective validation of disseminated intravascular coagulation diagnostic criteria for critically ill patients: comparing current criteria. Crit Care Med 2006;34:625-31.

[23] Kinasewitz GT, Zein JG, Lee GL, et al. Prognostic value of a simple evolving disseminated intravascular coagulation score in patients with severe sepsis. Crit Care Med 2005;33:2214-21.

[24] Madoiwa S, Nunomiya S, Ono T, et al. Plasminogen activator inhibitor 1 promotes a poor prognosis in sepsis-induced disseminated intravascular coagulation. Int J Hematol 2006;84:398-405.

[25] Abraham E, Singer M. Mechanisms of sepsis-induced organ dysfunction. Crit Care Med 2007;35:2408-16.

[26] Levi M, Schultz M. Coagulopathy and platelet disorders in critically ill patients. Minerva Anestesiol 2010;76:851-9.

[27] Crowther MA, Cook DJ, Meade MO, et al. Thrombocytopenia in medical-surgical critically ill patients: prevalence, incidence, and risk factors. J Crit Care 2005;20:348-53.

[28] Moreau D, Timsit JF, Vesin A, et al. Platelet count decline: an early prognostic marker in critically ill patients with prolonged ICU stays. Chest 2007;131:1735-41.

[29] Mavrommatis AC, Theodoridis T, Orfanidou A, et al. Coagulation system and platelets are fully activated in uncomplicated sepsis. Crit Care Med 2000;28:451-7.

[30] Zeerleder S, Hack CE, Wuillemin WA. Disseminated intravascular coagulation in sepsis. Chest 2005;128:2864-75.

[31] Madoiwa S, Tanaka H, Nagahama Y, et al. Degradation of cross-linked fibrin by leukocyte elastase as alternative pathway for plasmin-mediated fibrinolysis in sepsis-induced disseminated intravascular coagulation. Thromb Res 2011;127:349-55.

[32] Asakura H, Ontachi Y, Mizutani T, et al. Decreased plasma activity of antithrombin or protein C is not due to consumption coagulopathy in septic patients with disseminated intravascular coagulation. Eur J Haematol 2001;67:170-5.

[33] Mavrommatis AC, Theodoridis T, Economou M, et al. Activation of the fibrinolytic system and utilization of the coagulation inhibitors in sepsis: comparison with severe sepsis and septic shock. Intensive Care Med 2001;27:1853-9.

[34] Nilsson G, Astermark J, Lethagen S, et al. Protein C levels can be forecasted by global haemostatic tests in critically ill patients and predict long-term survival. Thromb Res 2005;116:15-24.

[35] Sakata Y, Loskutoff DJ, Gladson CL, et al. Mechanism of protein C-dependent clot lysis: role of plasminogen activator inhibitor. Blood 1986;68:1218-23.

[36] Bannach FG, Gutierrez-Fernandez A, Parmer RJ, et al. Interleukin-6-induced plasminogen gene expression in murine hepatocytes is mediated by transcription factor CCAAT/enhancer binding protein beta (C/EBPbeta). J Thromb Haemost 2004;2:2205-12.

[37] Gabay C, Kushner I. Acute-phase proteins and other systemic responses to inflammation. N Engl J Med 1999;340:448-54.

Suppression of lymph node and lung metastases of endometrial cancer by muscle-mediated expression of soluble vascular endothelial growth factor receptor-3

Kayoko Takahashi,[1,2,4] Hiroaki Mizukami,[1,3] Yasushi Saga,[2] Yuji Takei,[2] Masashi Urabe,[1] Akihiro Kume,[1] Shizuo Machida,[2] Hiroyuki Fujiwara,[2] Mitsuaki Suzuki[2] and Keiya Ozawa[1,3]

[1]Division of Genetics Therapeutics, Center for Molecular Medicine; [2]Department of Obstetrics and Gynecology, Jichi Medical University, Shimotsuke, Japan

Lymph node metastasis is the most important prognostic factor of endometrial cancer. However, effective therapy has not been established against lymph node metastasis. In this study, we explored the efficacy of gene therapy targeting lymph node metastasis of endometrial cancer by suppressing the action of vascular endothelial growth factor (VEGF)-C through soluble VEGF receptor-3 (sVEGFR-3) expression. For this purpose, we first conducted a model experiment by introducing sVEGFR-3 cDNA into an endometrial cancer cell line HEC1A and established HEC1A/sVEGFR-3 cell line with high sVEGFR-3 expression. The conditioned medium of HEC1A/sVEGFR-3 cells inhibited lymphatic endothelial cell growth in vitro, and sVEGFR-3 expression in HEC1A cells suppressed in vivo lymph node and lung metastases without inhibiting the growth of a subcutaneously inoculated tumor. To validate the therapeutic efficacy, adeno-associated virus vectors encoding sVEGFR-3 were injected into the skeletal muscle of mice with lymph node metastasis. Lymph node and lung metastases of HEC1A cells were completely suppressed by the muscle-mediated expression of sVEGFR-3 using adeno-associated virus vectors. These results suggest the possibility of gene therapy against lymph node and lung metastases of endometrial cancer by using muscle-mediated expression of sVEGFR-3. (Cancer Sci, doi: 10.1111/cas.12184, 2013)

E ndometrial cancer is the most commonly encountered gynecologic malignancy and the fourth most common malignant tumor in the USA.[1] Because this cancer is often detected at an early stage while it is still confined to the uterus, the overall survival rate exceeds 80%.[1] However, the prognosis of advanced endometrial cancer remains poor.[2,3] Although various attempts have been made to treat advanced endometrial cancer, including surgery, radiotherapy and multi-drug chemotherapy, satisfactory progress has not been achieved. In fact, overall treatment results in endometrial cancer have not improved over the past 30 years.[1] The most important prognostic factor in endometrial cancer is extra-uterine spread, especially lymph node and lung metastases.[4] Therefore, to improve the prognosis of endometrial cancer, it is necessary to develop effective therapy against such advanced conditions.

Factors related to lymphangiogenesis and lymph node metastasis have been clarified recently. Among these factors, vascular endothelial growth factor (VEGF)-C, which is the natural ligand for VEGF receptor-3 (VEGFR-3), is one of the most important. VEGF-C binds to VEGFR-3 and induces its tyrosine autophosphorylation. VEGF-C is specific to the lymphatic vascular system and mediates lymphangiogenesis.[5] In malignant tissues, the tumor cells and stromal cells promote VEGF-C secretion, thereby inducing lymphangiogenesis and lymph node metastasis.[6] The soluble form of VEGFR-3 (sVEGFR-3) is a potent inhibitor of VEGF-C signaling, which inhibits fetal lymphangiogenesis and induces regression of already formed lymphatic vessels.[7] Therefore, lymph node metastasis of a malignant tumor may be controlled by the action of sVEGFR-3.

Recently, we developed a murine model for lymph node metastasis using orthotopic injection of an endometrial cancer cell line.[8] Based on the study, we sought to investigate the efficacy of sVEGFR3 by its constitutive expression. For this purpose, the adeno-associated virus (AAV) vector is appropriate. The AAV is a widely–used vector derived from a non-pathogenic virus, and long-term transgene expression can be obtained following intramuscular injection.[9] We have reported the efficacy of muscle-mediated soluble Flt-1 expression using AAV vectors in both subcutaneous and intraperitoneally disseminated ovarian cancer.[10] In this study, we explored the efficacy of gene therapy against metastases of endometrial cancer by muscle-mediated expression of sVEGFR-3 using AAV vectors.

Materials and Methods

Cells and plasmids. The human endometrial cancer cell line HEC1A[11] was obtained from the Japanese Collection of Research Bioresources, where the cell line is authenticated by the Multiplex-PCR method using short tandem repeats.[12] The HEC1A was cultured in DMEM/F12 (GIBCO, Grand Island, NY, USA) supplemented with 10% inactivated FCS, 100 U/mL of penicillin and 100 µg/mL of streptomycin (GIBCO) at 37°C in a 5% CO_2 atmosphere. Human neonatal dermal lymphatic endothelial cells (LEC) were purchased from Angio-Bio (Del Mar, CA, USA) and maintained in EGM-MV2 BulletKit (Cambrex, East Rutherford, NJ, USA) supplemented with 10% inactivated FCS at 37°C in a 5% CO_2 atmosphere. All cell lines were maintained for less than 3 months after resuscitation. The cDNA of sVEGFR-3 was cloned by PCR using a human lung cDNA library (Stratagene, La Jolla, CA, USA) as a template, with the primers previously described.[7] Cloned sVEGFR-3 cDNA was inserted into the multi-cloning site (MCS) of pSecTagHygroB vector (Stratagene) to generate

a VEGFR-3-expression plasmid. A luciferase (LUC)-encoding plasmid was also constructed and used as a control vector. p2ITR-sVEGFR-3 is an sVEGFR-3 expression plasmid prepared by incorporating human sVEGFR-3 cDNA into the EcoRI site of pAAV-MCS (Stratagene).

Development of stably transduced cells. Either an sVEGFR3-expression or a LUC-expression plasmid was introduced into the HEC1A cells using the standard calcium phosphate precipitation method.[13] After transfection, the cells were cultured and selected in the presence of 200 μg/mL of hygromycin B (Invitrogen, Carlsbad, CA, USA). After 4 weeks, the hygromycin B-resistant HEC1A/sVEGFR-3 and HEC1A/LUC cell lines were established and maintained thereafter in the presence of 200 μg/mL of hygromycin B.

Adeno-associated virus vector production. Adeno-associated virus vectors were produced by triple-plasmid transfection to 293 cells (Stratagene) using p2ITR-sVEGFR-3, the helper plasmid for adenovirus genes,[14] and the helper plasmid for AAV1.[15,16] A plasmid encoding human coagulation factor IX (hfIX) gene was used to prepare the control AAV vector.[17] The vector stocks were purified using cesium chloride density-gradient ultracentrifugation, and the titer was determined by dot blot and real-time PCR, as described previously.[18] The primers were designed to amplify the cytomegalovirus promoter sequence, and the forward and reverse primers were 5'-GTA TTT ACG GTA AAC TGC CCA CTT-3' and 5'-AGT CCC ATA AGG TCA TGT ACT GG-3', respectively.

Vascular endothelial growth factor-C and soluble vascular endothelial growth factor receptor-3 quantitation. HEC1A, HEC1A/LUC and HEC1A/sVEGFR-3 cells were inoculated in 10-cm dishes and cultured in a 10% FCS-supplemented DMEM/F12 medium. When the cells grew to approximately 80% confluence, the culture supernatant was replaced with serum-free culture medium. After 48 h, the culture supernatant was recovered. The concentration of VEGF-C in the supernatant of HEC1A was determined using a Quantikine Human VEGF-C enzyme-linked immunosorbent assay kit (R&D Systems, Minneapolis, MN, USA). The concentrations of sVEGFR-3 in the supernatant of HEC1A, HEC1A/LUC and HEC1A/sVEGFR3 were determined by DuoSet Human VEGFR-3 (R&D Systems).

Lymphatic endothelial cells proliferation assay. Conditioned media were generated by culturing 1 × 10⁶ HEC1A/LUC cells or HEC1A/sVEGFR-3 cells in 2 mL of serum-free DMEM/F12 for 48 h. LEC (5 × 10³/well) were plated in 96-well plates in EGM-MV2 plus 5% FCS containing 50% of either conditioned medium with 100 ng/mL VEGF-C (R&D Systems). LEC proliferation was assessed by a colorimetric assay using Cell Proliferation Kit II (XTT; Boehringer Mannheim Biochemica, Mannheim, Germany) 48 h after plating.

Tumor cell transduction model: subcutaneously inoculated tumor growth. Four to six-week-old female BALB/c nude mice (Japan Clea Laboratories, Tokyo, Japan) were used in the experiment. HEC1A/LUC or HEC1A/sVEGFR-3 cells (5 × 10⁶) were subcutaneously transplanted into the backs of the mice, and tumor sizes were measured once a week using a micrometer caliper. Tumor volume was calculated using the formula: volume = (short diameter)² × (long diameter) × 0.5.[19]

Evaluation of metastasis. HEC1A/LUC or HEC1A/sVEGFR-3 cells (5 × 10⁶) were injected into the uterine cavities of pentobarbital sodium-anesthetized, laparotomized mice, as described previously.[8] After 8 weeks, metastatic lesions were thoroughly investigated and counted.

Therapeutic model using adeno-associated virus vector: evaluation of metastasis in orthotopically inoculated model. HEC1A cells (5 × 10⁶) were injected into the uterine cavities of pentobarbital sodium-anesthetized, laparotomized mice, as described previously.[8] At the same time AAV1-hfIX or AAV1-sVEGFR-

3 vector (2.5 × 10¹² genome copy) was injected into the hindlimb skeletal muscles of the mice. Eight weeks after injection, the metastatic changes were extensively investigated and numbers of enlarged lymph nodes and lung metastases were counted.

Statistical analysis. Intergroup differences were tested for significance using Student's *t*-test. A *P*-value <0.05 was considered significant.

Results

Detection of vascular endothelial growth factor-C and soluble vascular endothelial growth factor receptor-3 in culture supernatants. The concentration of VEGF-C in the culture supernatant of HEC1A cells was 235 ± 12 pg/mL. In the culture supernatant of HEC1A/sVEGFR-3 cells, 45.0 ± 3.2 pg/mL of sVEGFR-3 was detected, but no sVEGFR-3 was detected in the culture supernatant of either HEC1A or HEC1A/LUC cells.

Inhibitory effects of soluble vascular endothelial growth factor receptor-3 on *in vitro* lymphatic endothelial cells growth. The effect of the sVEGFR-3 expression of HEC1A/sVEGFR-3 cells on the action of VEGF-C was estimated using *in vitro* cultures of LEC. The number of LEC in EGM-MV2 culture medium, including 100 ng/mL recombinant VEGF-C plus 50% conditioned medium from HEC1A/sVEGFR-3 cells, was significantly smaller than that in the control (Fig. 1a–c, *P* < 0.01). We concluded that the mitogenic effect of VEGF-C on LEC was abrogated by the presence of sVEGFR-3 in the HEC1A/sVEGFR-3 conditioned medium.

Tumor cell transduction model: subcutaneously inoculated tumor growth. The tumor growth curves of HEC1A/LUC and HEC1A/sVEGFR-3 show no significant differences between the two groups (Fig. 2). This indicates that expression of sVEGFR-3 did not affect the growth of subcutaneously inoculated tumors.

Lymph node metastasis. The effects of sVEGFR-3 gene expression on lymph node metastasis *in vivo* are shown (Fig. 3a–c). The mean number of lymph node metastases 8 weeks after injection was 1.0 ± 0.7 in the control group, but no lymph node metastases were observed in the HEC1A/sVEGFR-3-injected group (Fig. 3c), indicating that sVEGFR-3 inhibited lymph node metastasis of the HEC1A cells.

Lung metastasis. After thorough investigation for metastasis, we noticed lung metastasis in these animals. Therefore, we focused on the number of lung metastases along with the number of lymph node metastases. The effects of sVEGFR-3 gene expression on lung metastasis *in vivo* are summarized in Figure 4. The mean number of lung metastases 8 weeks after injection was 3.8 ± 0.8 in the control group, but no lung metastases were observed in the HEC1A/sVEGFR-3-injected group, indicating that sVEGFR-3 completely inhibited lung metastasis of the HEC1A cells.

Therapeutic model using adeno-associated virus vector. The efficacy of muscle-mediated sVEGFR-3 expression was evaluated in lymph node and lung metastases models using HEC1A cells. As shown in Figure 5, the mean number of lymph node metastases 8 weeks after injection of HEC1A cells was 2.4 ± 0.5 in the control group, while no lymph node metastases were observed in the AAV1-sVEGFR-3-injected group. Moreover, the mean number of lung metastases 8 weeks after injection of HEC1A cells was 5.7 ± 2.1 in the control group, while no lung metastases were observed in the AAV1-sVEGFR-3-injected group (Fig. 6a–c). Thus, we observed a significant therapeutic effect in both lymph node and lung metastases.

Discussion

In this study, we explored the possibility of gene therapy targeted at lymph node and lung metastasis using muscle-mediated expression of sVEGFR-3 as a new treatment modality

2

for advanced endometrial cancer. Our results show that sVEGFR-3 in the conditioned medium of sVEGFR-3-transduced endometrial cancer cells inhibited LEC growth *in vitro*, and sVEGFR-3 expression in endometrial cancer cells suppressed
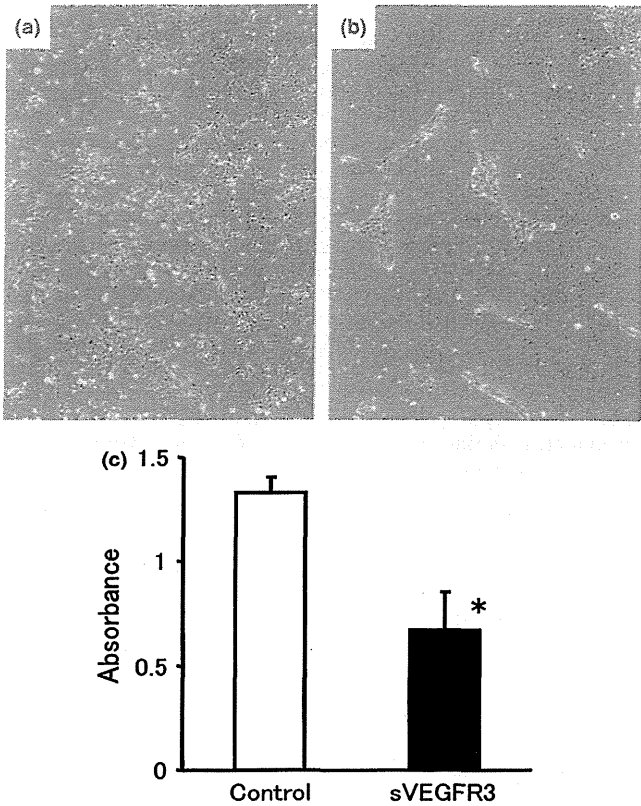

Fig. 1. Suppression of vascular endothelial growth factor (VEGF)-C-driven lymphatic endothelial cell (LEC) proliferation by conditioned medium of soluble vascular endothelial growth factor receptor-3 (sVEGFR-3)-expressing cells. Cells were plated at 5×10^3 cells/well in 96-well plates, and 50% sVEGFR-3-conditioned medium or luciferase-conditioned medium was added with 100 ng/mL recombinant human VEGF-C. The number of LEC with 50% sVEGFR-3-conditioned medium (b) was clearly smaller than that with control (a). The cells were counted by colorimetric assay 48 h after plating. Each bar represents the mean ± SD. (*P < 0.01) (c).
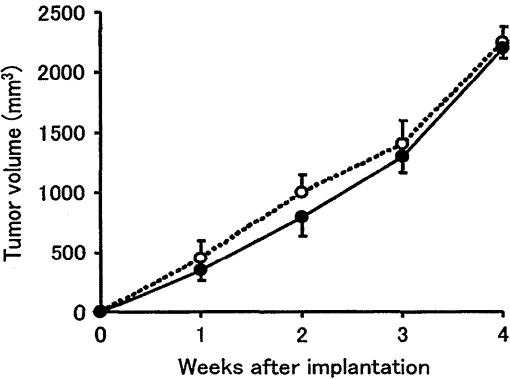
Fig. 2. The tumor growth curves of HEC1A/luciferase and HEC1A /vascular endothelial growth factor receptor-3. Tumor cells were subcutaneously injected into the backs of mice, and the sizes of tumors were measured every week. There were no significant differences between the two groups. Each bar represents the mean ± SD.
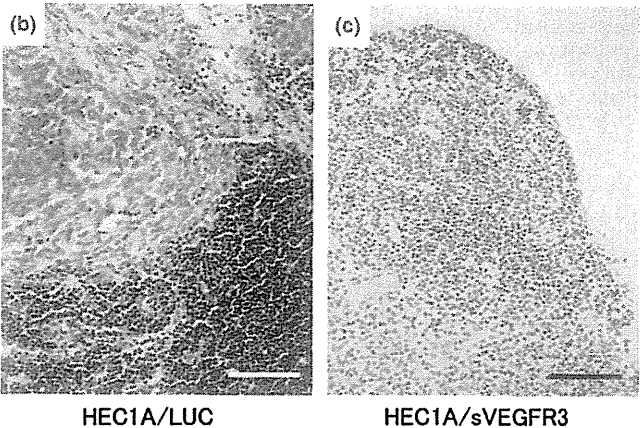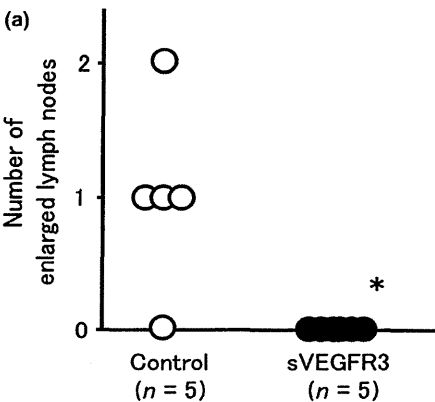

HEC1A/LUC   HEC1A/sVEGFR3

Fig. 3. (a) The number of lymph node metastases 8 weeks after injection of HEC1A/luciferase and HEC1A/vascular endothelial growth factor receptor-3 (sVEGFR-3) cells. Lymph node metastases were observed in the control group (b), while no lymph node metastases were observed in the HEC1A/sVEGFR-3-injected group (c). The mean number of lymph node metastases was 1.0 ± 0.7 in the control group, while no lymph node metastases were observed in the HEC1A/sVEG-FR-3-injected group. Bars represent 100 μm.
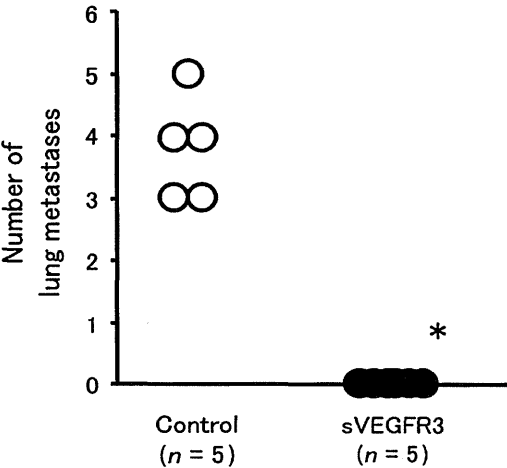

Fig. 4. The number of lung metastases 8 weeks after injection of HEC1A/luciferase and HEC1A/vascular endothelial growth factor receptor-3 (sVEGFR-3) cells. The mean number of lung metastases 8 weeks after injection was 3.8 ± 0.8 in the control group, while no lung metastases were observed in the HEC1A/sVEGFR-3-injected group.
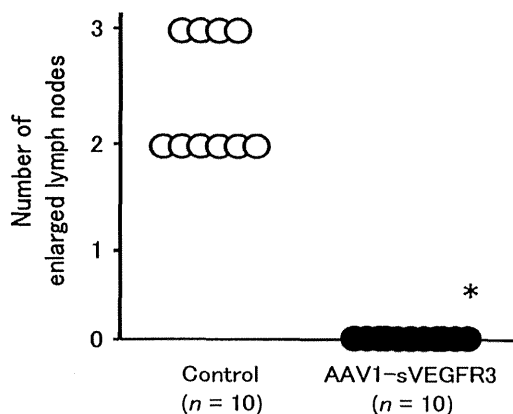
Takahashi *et al.*

Fig. 5. The number of lymph node metastases 8 weeks after injection of HEC1A cells in the mice that had received intramuscular injections of AAV1-sVEGFR-3 or control vector. The mean number of lymph node metastases was 2.4 ± 0.5 in the control group, while no lymph node metastases were observed in the AAV1-sVEGFR-3-injected group. sVEGFR-3, vascular endothelial growth factor receptor-3.
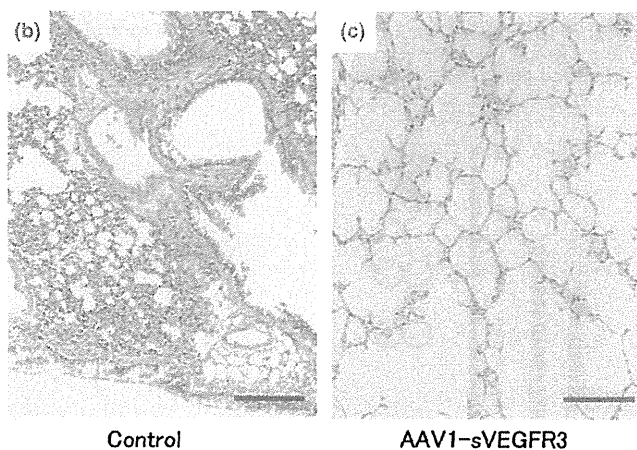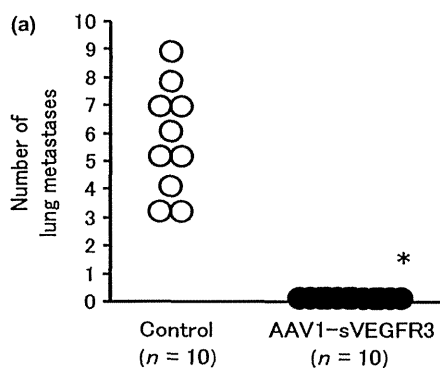

Fig. 6. Lung metastases 8 weeks after injection of HEC1A cells in the mice that had received intramuscular injections of AAV1-sVEGFR-3 or control vector. The mean number of lung metastases was 5.7 ± 2.1 in the control group, while no lung metastases were observed in the AAV1-sVEGFR-3-injected group (a). Lung metastases were observed in the control group (b), while no lung metastases were observed in the AAV1-sVEGFR-3-injected group (c). Bars represent 100 μm. sVEGFR-3, vascular endothelial growth factor receptor-3.

in vivo lymph node and lung metastases, although it did not inhibit the growth of subcutaneously inoculated tumors. In addition, lymph node and lung metastases of endometrial cancer cells were suppressed by muscle-mediated expression of sVEGFR-3 using AAV vectors.

Lymph node metastasis is the most important prognostic factor in endometrial cancer.[3,20] In this study, we tested the efficacy of a gene therapy strategy using sVEGFR-3 to suppress lymph node metastasis through VEGF-C inhibition. We first introduced sVEGFR-3 cDNA into an endometrial cancer cell line HEC1A and established a cell line (HEC1A/s VEGFR-3) with high expression of sVEGFR-3 to investigate its function. The growth of HEC1A/sVEGFR-3 did not show any difference in either in vitro cell proliferation (data not shown) or in vivo tumor expansion (Fig. 2), showing that overexpression of sVEGFR-3 did not influence the spread of endometrial cancer per se. In contrast, in the lymph node metastasis model using HEC1A/sVEGFR-3, lymph node metastasis was completely suppressed. Moreover, in this model, lung metastasis was also completely eliminated. Thus, we demonstrated that expression of sVEGFR-3 could control lymph node and lung metastases of endometrial cancer. Because the expression of sVEGFR-3 did not influence the growth of HEC1A cells, its action was confined to the suppression of lymph node metastasis. The VEGF-C in culture supernatant is thought to be derived from HEC1A cells, and accumulated during cell culture. In fact, we demonstrated various but similar concentrations of VEGF-C in tumor cell culture supernatant.[8] In contrast, soluble VEGFR3 was demonstrated specifically to the cells transduced by sVEGFR3 gene, as shown in the Results section.

Based on these findings, we aimed to establish a gene therapy using sVEGFR-3. For this purpose, we compared the utility of candidate vectors to attain this goal. Non-viral vectors are easier to prepare, and may be safer, but the efficacy is much weaker than viral vectors. Successful in vivo delivery has been limited.[21] As for the viral vectors, many successful outcomes in clinical trials have been reported.[22] For the current study, we chose an AAV1-based vector, as it appears to be the most efficient in muscle transduction.[9,15,23] The result was that both lymph node and lung metastases of endometrial cancer cells were completely suppressed by muscle-mediated expression of sVEGFR-3. These results suggest the possibility of gene therapy targeting lymph node and lung metastases of endometrial cancer by muscle-mediated expression of sVEGFR-3. In the case of AAV vectors, a couple of weeks may be necessary for maximal transgene expression.[22,24–26] Nonetheless, as sufficient levels of expression can last over the observation period of 8 weeks, a significant outcome was obtained even when the vector was administered simultaneously to the tumor inoculation. In this study, we selected muscle tissue for gene expression. For the clinical translation, other tissues may be more appropriate: for example, liver can be efficiently targeted by AAV8 vector[26] and adipose tissue can be targeted by AAV1 vectors.[24]

This study aimed to suppress actions of VEGF-C through the expression of a soluble form of its receptor, sVEGFR3. Therefore, lymph node metastasis was suppressed as a result of lymphangiogenesis inhibition. However, because this treatment did not suppress primary tumor growth, it may be necessary to combine it with other treatment modalities such as surgery and chemotherapy in clinical practice. One recent study utilized chemotherapeutic reagents in addition to gene therapy using soluble VEGF receptors for prolonged survival in mice.[27]

Recently, we developed a lymph node metastasis model using orthotopic injection of endometrial cancer.[8] In that report, only lymph node metastasis was noted. During the current series of experiments, metastatic foci of the lungs could barely be recognized from the surface, and we noticed lung metastasis after extensive microscopic examination.

4

Therefore, the number of metastasis was counted based on the microscopic examination of the tissue sections. As for lung metastasis, both lymphatic and hematogenous routes are known. It is not easy to determine the route of metastasis solely by histopathological examination. Nonetheless, we assume that in human endometrial cancer, the main route of lung metastasis is lymphatic as lymph node metastasis is detected in more than half of the patients with lung metastasis.[28] Also, in the present study, lung metastasis of endometrial cancer was completely suppressed as a result of controlling lymph node metastasis with sVEGFR-3.

In this study, we demonstrated the efficacy of sVEGFR-3 at one vector dose. As both lymph node and lung metastasis were completely eliminated, there is a possibility that the therapeutic efficacy can be demonstrated at lower vector doses. In addition, in our observation, no side effects were noted in the mice, including in behavior, body weight and muscle tissue. However, for application to human therapy, these points need to be clarified in more detail.

Few studies concerning molecular-targeted therapy or gene therapy for endometrial cancer have been reported. Gene therapy against lymph node and lung metastases, which we propose here, could be beneficial for patients with advanced endometrial cancer. New therapeutic modalities, including this one, are expected to result in improved outcomes for endometrial cancer.

Disclosure Statement

The authors have no conflict of interest to declare.

References

1 Siegel R, Ward E, Brawley O, Jemal A. Cancer statistics, 2011: the impact of eliminating socioeconomic and racial disparities on premature cancer deaths. *CA Cancer J Clin* 2011; **61**: 212–36.
2 Amant F, Moerman P, Neven P, Timmerman D, Van Limbergen E, Vergote I. Endometrial cancer. *Lancet* 2005; **366**: 491–505.
3 Wolfson AH, Sightler SE, Markoe AM *et al.* The prognostic significance of surgical staging for carcinoma of the endometrium. *Gynecol Oncol* 1992; **45**: 142–6.
4 Lurain J. Uterine cancer. In: Berec J, ed. *Novak's Gynecology*, 12th edn. Baltimore: Williams & Wilkins, 1996; 1057–77.
5 Makinen T, Veikkola T, Mustjoki S *et al.* Isolated lymphatic endothelial cells transduce growth, survival and migratory signals via the VEGF-C/D receptor VEGFR-3. *EMBO J* 2001; **20**: 4762–73.
6 Skobe M, Hawighorst T, Jackson DG *et al.* Induction of tumor lymphangiogenesis by VEGF-C promotes breast cancer metastasis. *Nat Med* 2001; **7**: 192–8.
7 Makinen T, Jussila L, Veikkola T *et al.* Inhibition of lymphangiogenesis with resulting lymphedema in transgenic mice expressing soluble VEGF receptor-3. *Nat Med* 2001; **7**: 199–205.
8 Takahashi K, Saga Y, Mizukami H *et al.* Development of a mouse model for lymph node metastasis with endometrial cancer. *Cancer Sci* 2011; **102**: 2272–7.
9 Mueller C, Flotte TR. Clinical gene therapy using recombinant adeno-associated virus vectors. *Gene Ther* 2008; **15**: 858–63.
10 Takei Y, Mizukami H, Saga Y *et al.* Suppression of ovarian cancer by muscle-mediated expression of soluble VEGFR-1/Flt-1 using adeno-associated virus serotype 1-derived vector. *Int J Cancer* 2007; **120**: 278–84.
11 Kuramoto H, Tamura S, Notake Y. Establishment of a cell line of human endometrial adenocarcinoma in vitro. *Am J Obstet Gynecol* 1972; **114**: 1012–9.
12 Tanabe H, Takada Y, Minegishi D, Kurematsu M, Masui T, Mizusawa H. Cell line individualization by STR multiplex system in the cell bank found cross contamination between ECV304 and EJ-1/T24. *Tiss Cult Res Commun* 1999; **18**: 329–38.
13 Takei Y, Saga Y, Mizukami H *et al.* Overexpression of PTEN in ovarian cancer cells suppresses i.p. dissemination and extends survival in mice. *Mol Cancer Ther* 2008; **7**: 704–11.
14 Matsushita T, Elliger S, Elliger C *et al.* Adeno-associated virus vectors can be efficiently produced without helper virus. *Gene Ther* 1998; **5**: 938–45.

15 Mochizuki S, Mizukami H, Kume A *et al.* Adeno-associated virus (AAV) vector-mediated liver- and muscle-directed transgene expression using various kinds of promoters and serotypes. *Gene Ther Mol Biol* 2004; **8**: 9–18.
16 Xiao W, Chirmule N, Berta SC, McCullough B, Gao G, Wilson JM. Gene therapy vectors based on adeno-associated virus type 1. *J Virol* 1999; **73**: 3994–4003.
17 Ogura T, Mizukami H, Mimuro J *et al.* Utility of intraperitoneal administration as a route of AAV serotype 5 vector-mediated neonatal gene transfer. *J Gene Med* 2006; **8**: 990–7.
18 Ishiwata A, Mimuro J, Mizukami H *et al.* Liver-restricted expression of the canine factor VIII gene facilitates prevention of inhibitor formation in factor VIII-deficient mice. *J Gene Med* 2009; **11**: 1020–9.
19 Kung AL, Wang S, Klco JM, Kaelin WG, Livingston DM. Suppression of tumor growth through disruption of hypoxia-inducible transcription. *Nat Med* 2000; **6**: 1335–40.
20 Lurain JR, Rice BL, Rademaker AW, Poggensee LE, Schink JC, Miller DS. Prognostic factors associated with recurrence in clinical stage I adenocarcinoma of the endometrium. *Obstet Gynecol* 1991; **78**: 63–9.
21 Zhang Y, Satterlee A, Huang L. In vivo gene delivery by nonviral vectors: overcoming hurdles? *Mol Ther* 2012; **20**: 1298–304.
22 Giacca M, Zacchigna S. Virus-mediated gene delivery for human gene therapy. *J Control Release* 2012; **161**: 377–88.
23 Chao H, Liu Y, Rabinowitz J, Li C, Samulski RJ, Walsh CE. Several log increase in therapeutic transgene delivery by distinct adeno-associated viral serotype vectors. *Mol Ther* 2000; **2**: 619–23.
24 Mizukami H, Mimuro J, Ogura T *et al.* Adipose tissue as a novel target for in vivo gene transfer by adeno-associated viral vectors. *Hum Gene Ther* 2006; **17**: 921–8.
25 Flotte TR, Trapnell BC, Humphries M *et al.* Phase 2 clinical trial of a recombinant adeno-associated viral vector expressing alpha1-antitrypsin: interim results. *Hum Gene Ther* 2011; **22**: 1239–47.
26 Nathwani AC, Tuddenham EG, Rangarajan S *et al.* Adenovirus-associated virus vector-mediated gene transfer in hemophilia B. *N Engl J Med* 2011; **365**: 2357–65.
27 Sopo M, Anttila M, Sallinen H *et al.* Antiangiogenic gene therapy with soluble VEGF-receptors -1, -2 and -3 together with paclitaxel prolongs survival of mice with human ovarian carcinoma. *Int J Cancer* 2012; **131**: 2394–401.
28 Otsuka I, Ono I, Akamatsu H, Sunamori M, Aso T. Pulmonary metastasis from endometrial carcinoma. *Int J Gynecol Cancer* 2002; **12**: 208–13.

Prophylaxis and Treatment of Alzheimer's Disease by Delivery of an Adeno-Associated Virus Encoding a Monoclonal Antibody Targeting the Amyloid Beta Protein

Masaru Shimada[1], Shinya Abe[1], Toru Takahashi[1], Kazumasa Shiozaki[2], Mitsue Okuda[3], Hiroaki Mizukami[4], Dennis M. Klinman[5], Keiya Ozawa[4], Kenji Okuda[1]*

1 Department of Molecular Biodefense Research, Yokohama City University, Yokohama, Kanagawa, Japan, 2 Department of Psychiatry, Yokohama City University, Yokohama, Kanagawa, Japan, 3 Okuda Dental Clinic, Yokohama, Kanagawa, Japan, 4 Division of Genetic Therapeutics, Center for Molecular Medicine, Jichi Medical School, Tochigi-ken, Japan, 5 Laboratory of Experimental Immunology, Cancer and Inflammation Program, National Cancer Institute, National Institutes of Health, Frederick, Maryland, United States of America

Abstract

We previously reported on a monoclonal antibody (mAb) that targeted amyloid beta (Aß) protein. Repeated injection of that mAb reduced the accumulation of Aß protein in the brain of human Aß transgenic mice (Tg2576). In the present study, cDNA encoding the heavy and light chains of this mAb were subcloned into an adeno-associated virus type 1 (AAV) vector with a 2A/furin adapter. A single intramuscular injection of 3.0×10^{10} viral genome of these AAV vectors into C57BL/6 mice generated serum anti-Aß Ab levels up to 0.3 mg/ml. Anti-Aß Ab levels in excess of 0.1 mg/ml were maintained for up to 64 weeks. The effect of AAV administration on Aß levels in vivo was examined. A significant decrease in Aß levels in the brain of Tg2576 mice treated at 5 months (prophylactic) or 10 months (therapeutic) of age was observed. These results support the use of AAV vector encoding anti-Aß Ab for the prevention and treatment of Alzheimer's disease.

Introduction

Alzheimer's disease (AD) is a disorder characterized by a diffuse loss of neurons and the accumulation of amyloid beta (Aß) protein, followed by the production of tau protein or senile plaques in the brain [1–2]. Active immunization with Aß peptide was found to reduce the amyloid burden and improve cognitive behavior in murine AD models [3–4].

Clinical trials involving peptide immunization were suspended owing to the development of meningoencephalitis in some volunteers vaccinated with Aß peptide [5–6]. Clinical studies and autopsy results indicated aseptic meningoencephalitis, presumably induced by the T-cell responses [6–8]. Of note, several of the samples obtained from vaccinated patients demonstrated a remarkable reduction in Aß protein levels and senile plaque formation [9–10]. These results suggest that if the adverse side effects of such therapy could be avoided, immune mediated elimination of Aß protein could represent a promising therapy for AD.

Based on these observations, the efficacy of intravenous delivery of humanized monoclonal antibodies (mAbs) against Aß was examined [11–13]. Despite the widespread reduction in Aß plaques, the passive transfer of mAb reduced AD-like symptoms in only a subset of patients [10]. This observation suggests that neuronal degeneration may occur during the early stages of AD, before the appearance of large Aß aggregates. Thus, it is important to eliminate Aß oligomers at the earliest stages of AD. Previously, we developed a mAb targeting the Aß1–13 peptide. Prophylactic delivery of this mAb or its F(ab')2 fragments to human Aß transgenic mice (Tg2576) effectively prevented the accumulation of Aß protein and plaques [14]. However, Pfeifer et al. [15] reported that anti-Aß mAb treatment could also lead to microhemorrhages in APP23 mice. Moreover, repeated high-dose mAb injections are likely to be very expensive [5,8].

A potentially safer and more efficacious strategy would be to inject an adeno-associated virus (AAV) that leads to the continuous production of anti-Aß mAb over an extended period. AAV is a nonpathogenic and poorly immunogenic virus. When used as a vector, it can transfer a gene of interest to non-dividing mammalian cells resulting in persistent transgene expression [16].

This work examines the feasibility of using an AAV vector type 1 (AAV vector) modified to encode the anti-Aß Ab to prevent or treat AD in mice. This approach avoids the need to repeatedly administer high doses of mAb. Results suggest that therapy with an Aß mAb-expressing AAV vector greatly reduce Aß accumulation in AD model mice.

Results

Production of Ab by cells transfected with the Aβ mAb – expressing AAV vector

We first determined whether the transduction of the new Aβ mAb – expressing AAV vector resulted in the production of mAb by HEK293 cells. As shown in Figure 1, we detected Abs in the cell lysates and culture supernatant of the transduced cells. Heavy (H) and Light (L) chains of the appropriate molecular weight were detected. In addition, we detected intact Ab under non – reducing condition. These results indicate that Aβ mAb – expressing AAV vector-transduced cells produce proteins with the molecular weight of Abs.

Binding activity of the Ab produced by AAV vector – transduced cells

We next assessed whether the HEK293 – derived Abs could bind to monomeric Aβ protein and oligomerized Aβ protein similar to those found in the brain of patients with AD [17]. Results show that culture supernatant derived from Aβ mAb-expressing AAV vector-transduced HEK293 cells bound to monomers, dimers, trimers, and tetramers of Aβ protein (Figure 2A).

We then analyzed whether Aβ mAb – expressing vector-produced Abs bound to Aβ aggregates by observing sliced brain sections from Tg2576 mice. Aβ aggregates were clearly detected in the brain sections using a polyclonal antibody against Aβ1 – 42, anti – Aβ1–13 mAb (IIA2), and the culture supernatant from Aβ mAb – expressing vector – transduced HEK293 cells (Figure 2B). These results suggest that functional anti-Aβ mAb is produced by cells transduced with this Aβ mAb – expressing vector.

Inhibition of hippocampal cell death by Aβ aggregates using culture supernatant from AAV-transduced cells

It is hypothesized that early AD is characterized by the aggregation of Aβ protein, and is followed by abnormal tau phosphorylation leading to massive neuronal cell death in the brain. We therefore examined whether the culture supernatant from Aβ mAb - expressing AAV vector-transduced cells could inhibit the death of primary hippocampal cells. As shown in Figure 3, synthetic soluble Aβ aggregates killed hippocampal cells.

This cell death was significantly reduced by the addition of culture supernatant from Aβ mAb - expressing vector-transduced cells at 6 h and 24 h after incubation. These results suggest that the culture supernatant of AAV-transduced cells can inhibit the death of primary hippocampal cells.

Antibody titers of mice infected with the Aβ mAb-expressing AAV vector

Ten weeks old C57BL/6 mice were intramuscularly (i.m.) injected with 3.0×10^9, 3.0×10^{10} or 3.0×10^{11} viral genome (vg) of the Aβ mAb - expressing vector or 3.0×10^{11} vg of LacZ-expressing vector. After administration, serum from these mice was collected monthly and antibody titers were assayed for 64 weeks (Figure 4). Anti-Aβ Ab titers peaked approximately 4 weeks after administration and then slowly declined, remaining detectable through 64 weeks of follow up. Ab titers were dose-dependent, with the greatest amount of Ab being present in mice treated with 10^{11} vg of the Aβ mAb-expressing AAV vector. In contrast, no Aβ-specific Abs were detected in mice injected with the LacZ-expressing AAV vector (data not shown). By 64-week post administration, 0.1 mg/ml of Aβ-specific Ab can be detected in the mice administrated with 3.0×10^{10} vg of the Aβ mAb-expressing AAV vector. Considering the safe dosage range of $2.1 \times 10^{12} - 6.9 \times 10^{13}$ vg/individual [18] and $2 \times 10^{11} - 1.8 \times 10^{12}$ vg/kg [19] in phase 1 clinical trials of intramuscular injection of the recombinant AAV vector, we use the dose of 3.0×10^{10} vg/mouse for further in vivo study, based on the body weight ratio of human beings (60 kg) vs mouse (20 g) and the Ab titer after administration of Aβ mAb-expressing AAV vector (Figure 4).

Effect of Aβ mAb-expressing AAV vector prophylaxis on Tg2576 mice

To determine whether the Aβ mAb-expressing AAV vector was able to prevent Tg2576 mice from developing AD, 5-month old animals were injected once with 3.0×10^{10} vg of this vector. Whereas no Aβ protein accumulated in normal mice, there was a statistically significant increase in the amount of Aβ1-40 and Aβ1-42 present in the brain of Tg2576 animals treated with the control LacZ-expressing vector by 10 months of age. The accumulation of this protein continued to rise over time (Figure 5B). By comparison, the amount of Aβ protein present

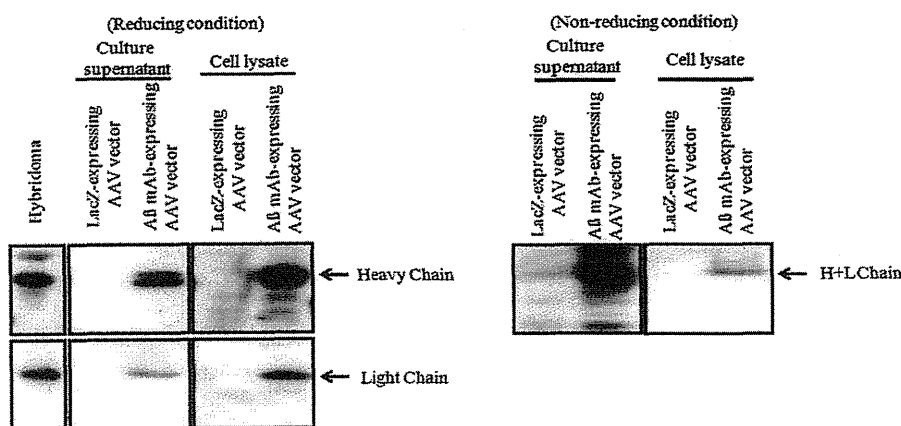**Figure 1. In vitro expression of anti - Aβ Abs following the transduction of HEK293 cells with the Aβ mAb – expressing AAV vector.** Western blots of culture supernatant and cell lysates identify the Ig light and heavy chain (under reducing conditions) and whole Ab (under non-reducing conditions). Cells transfected with a LacZ encoding AAV vector served as negative controls.
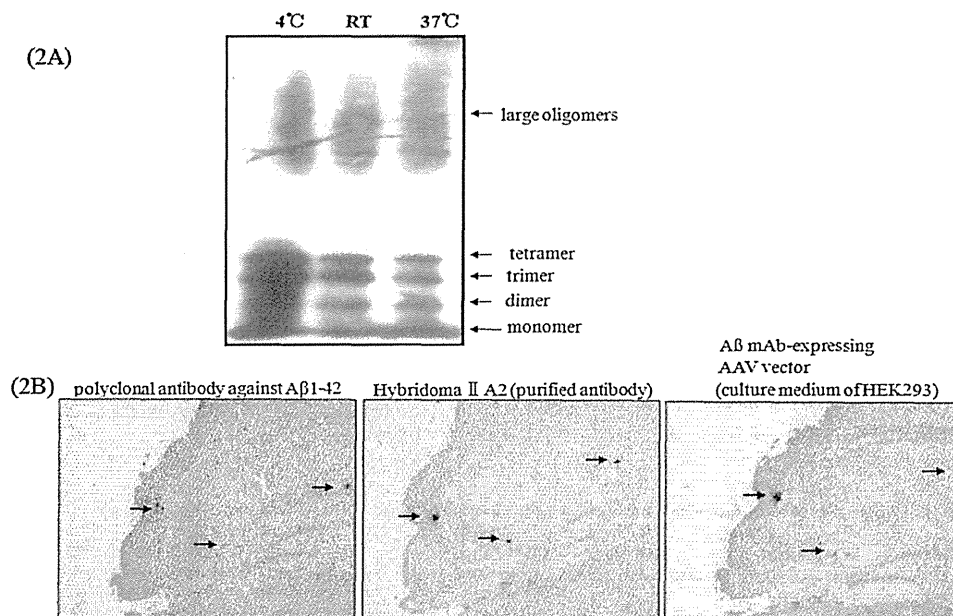doi:10.1371/journal.pone.0057606.g001

Figure 2. Binding activity of the Ab produced by Aβ mAb – expressing AAV vector-transduced cells. A) Binding of Ab from Aβ mAb – expressing AAV vector transduced HEK293 cells to synthetic Aβ peptides, monomers and oligomers by Western blot. The Ab1-42 peptide was aggregated at 4°C, room temperature (R.T.), or 37°C as described in Materials and Methods and detected by culture supernatant derived from Aβ mAb – expressing AAV vector transduced HEK293 cells. B) Anti – Aβ Ab derived from transduced HEK293 bound to Aβ plaques in 16-month old Tg2576 mice. The specificity of this binding was confirmed by use of polyclonal and monoclonal Abs (see details in Materials and Methods).
doi:10.1371/journal.pone.0057606.g002

in Tg2576 mice treated with the Aβ mAb-expressing AAV vector was significantly and persistently reduced (Figure 5B).

Serial sagital sections were prepared from the brains of these animals. Aβ protein deposits were then visualized immunohisto-chemically in these sections. Both the size and number of Aβ protein containing deposits increased over time in Tg mice treated with the LacZ-expressing vector. The number of such plaques was significantly reduced among mice treated with the Aβ mAb-expressing vector (Figure 5C).

Effect of Aβ mAb-expressing AAV vector treatment on Tg2576 mice

We finally sought to determine whether the Aβ mAb-expressing AAV vector could be used therapeutically. Ten-month old animals were injected with 3.0×10^{10} vg of vector. Aβ protein continued to accumulate at 13 months in mice treated with either the LacZ or Aβ mAb-expressing AAV vector. However by 15 months (and continuing through 17 months) the size and number of Aβ protein containing deposits in the brains of animals treated with the Aβ mAb-expressing vector was significantly reduced when compared to LacZ controls (Figure 6B). This divergence was confirmed
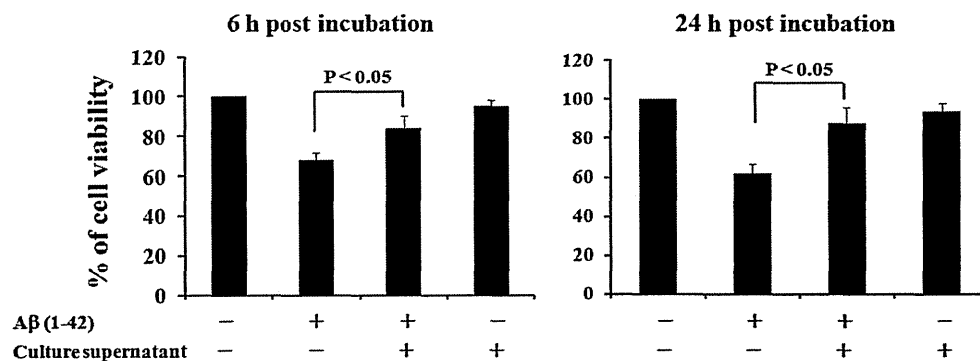
Figure 3. In vitro cytotoxicity inhibition test using primary culture hippocampal cells. The viability of primary hippocampal cells after 6–24 h of culture with 10 uM aggregated Aβ protein was examined. The effect of adding culture supernatant from Aβ mAb - expressing AAV vector transduced cells was also examined by MTT assay. Data represent the results of 5–8 independently analyzed samples and are presented as mean ± SE.
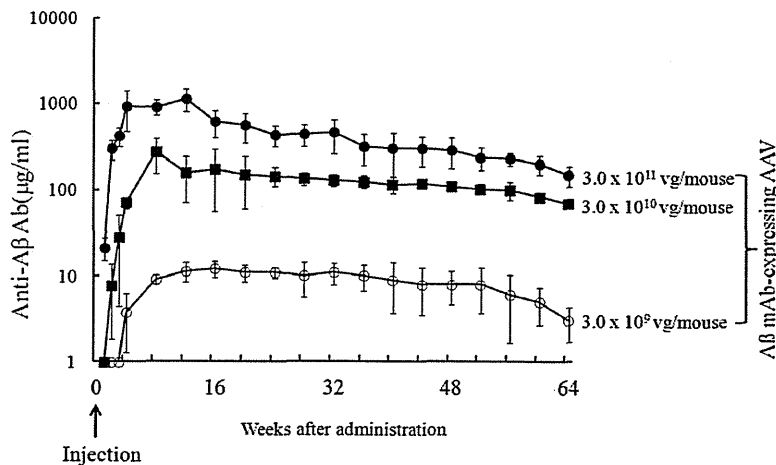doi:10.1371/journal.pone.0057606.g003

Figure 4. Kinetics of anti-Aβ Ab production by mice injected with Aβ mAb-expressing AAV. Normal C57BL/6 mice (n = 10/group) received a single intramuscular injection with 3.0×10^9, 3.0×10^{10}, 3.0×10^{11} vg of Aβ mAb-expressing AAV or 3.0×10^{11} vg of LacZ-expressing AAV vector. The titer of IgG1 Ab binding to Aβ1–42 was detected at indicated time points. Significant difference among groups received 3×10^9, 3×10^{12} and 3×10^{11} vg of Aβ mAb-expressing AAV was observed from 2-week to 64-week after administration (P<0.05). Data are presented as mean ± SE. doi:10.1371/journal.pone.0057606.g004

Discussion

Efforts to treatment AD patients with anti-Aβ Abs or through Aβ peptide vaccination provided novel insights concerning the pathogenesis of AD and opened new approaches to disease therapy. In an effort to overcome limitations of earlier strategies, the current work examined the effect of delivering an Aβ mAb - expressing AAV vector to Tg2576 mice (a murine model of AD). Prophylactic treatment of young (5 months) and therapeutic treatment of older (10 months) animals resulted in a significant and prolonged decrease in the amount of Aβ protein accumulating in the brain (Figure 5 and 6).

The AAV vector encoded an anti-Aβ mAb that bound to synthetic Aβ peptides and to senile plaques present in the brains of Tg2576 mice (Figure 1 and 2). Of interest, a single 3.0×10^{10} vg dose of the Aβ mAb-expressing AAV vector resulted in the production of Ab that persisted through the 64-week experimental period (Figure 4). As repeated injection of free anti-Aβ mAb can have negative consequences [15], the continuous production of Ab by cells transfected in vivo may provide an ideal method for AD prophylaxis and treatment.

Previous studies investigated the utility of AAV vector for the molecular therapy of Alzheimer's disease. Those vectors encoding antigen, Ab or other factors of potential therapeutic value were examined in various animal models [20–31]. These included studies of AAV vector expressing a single-chain variable fragment (scFv) antibody against Aβ protein for AD therapy [22–26]. Those studies showed that the scFv fragment had a much shorter serum half-life than whole Ab (7–14 hrs vs 20 days) [32], such that the scFv fragment was more suited for intracranial delivery rather than systemic delivery [22–26]. Delivery of scFv - expressing AAV vector intracranially reduced/prevented the formation of Aβ brain plaques and improved cognitive function in AD mice [22–26], while the delivery method is likely to raise safety issues.

This study examined the effect of treating 5- or 10-month old Tg2576 mice with the Aβ mAb - expressing AAV vector. Of

importance, a significant decline in the concentration of Aβ was found in the brains of both groups of recipient mice (monitored by ELISA and immunohistochemistry). The level of decline was similar in both groups despite the difference in when treatment was initiated (Figure 5 and 6). This may reflect the level of Aβ protein being so low in young mice that the effect of therapy cannot be detected until the animals reach 15 months of age. By that time the vector had been active in both treatment groups for a sufficient period to significantly reduce the accumulation of Aβ protein

Clinical trials showed that vaccination of AD patients with an Aβ peptide reduced the deposition of Aβ in some individuals [10]. Unfortunately, this treatment also led to the development of cerebroencephalitis in some patients, a side effect so severe that further development of this type of therapy was abandoned [11,14,33]. An alternative approach involved the intravenous administration of Abs against Aβ peptide [5,8]. While effective at reducing the accumulation of Aβ aggregates, the injection of anti-Aβ Ab resulted in a high incidence of cerebral microhemorrhages [15]. Approximately 30% of AD patients have cerebral amyloid angiopathy (CAA)-associated microhemorrhages [34]. Shroeter et al. [35] reported that anti-Aβ Ab treatment of 12-month old AD model mice resulted in a dose-dependent reduction of the occurrence of CAA after treatment. In older model mice, CAA is known to be relatively abundant [36–37]; however, the injection of a small amount of anti-Aβ mAb did not increase the incidence of microhemorrhages [36–37], indicating that long-lasting expression of anti-Aβ mAb by AAV vector may have some advantages in reducing the incidence of microhemorrhages. Many reports have explored the T-cell response after virus or non-virus-based vaccine against Alzheimer's. The T-cell response is very low or undetectable [38–40]. In this study, we have not explored the T-cell response, because our AAV vector expresses anti-Aβ-antibody, but not an antigen. Furthermore, we histologically evaluated the appearance of microhemorrhages and inflammation of brain in the mice treated with the Aβ mAb-expressing AAV vector. No evidence of this adverse side effect was observed even in 17-month old Tg2576 mice (data not shown).
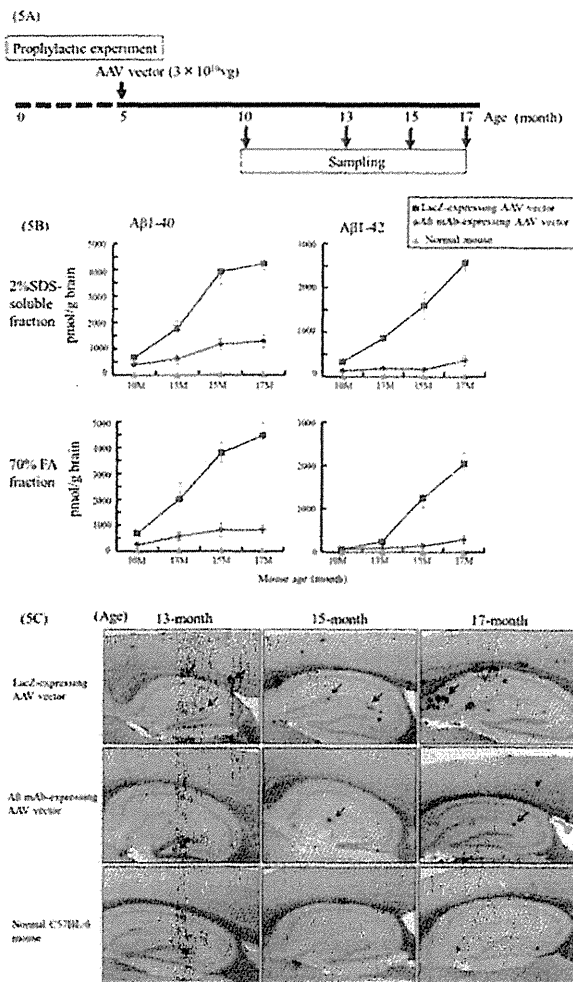
—310—

Figure 5. Prophylaxis of AD using Aß mAb-expressing AAV vector. Five-month old Tg2576 mice were injected i.m. with 3×10^{10} Aß mAb-expressing AAV. (A) Scheme of experiment. (B) The amount of Aß protein in brain extracts was determined using anti-Aß Ab-coated ELISA plates at age 10-, 13-, 15- and 17-month old (4–5 mice per time point). C57BL/6 mice were used as controls. Data are presented as mean ± SE. (C) Brain sections from Tg2576 or C57BL/6 mice were examined for Aß deposits by immunohistostaining using rabbit anti-human beta amyloid 1–42 polyclonal antibody.
doi:10.1371/journal.pone.0057606.g005

Figure 6. Therapy of AD using Aß mAb-expressing AAV vector. Tem-month old Tg2576 mice were injected i.m. with 3.0×10^{10} vg of the Aß mAb - expressing AAV vector. (A) Scheme of experiment. (B) The amount of Aß protein in brain extracts was determined using anti-Aß Ab-coated ELISA plates at age 10-, 13-, 15- and 17-month old (4–5 mice per time point). C57BL/6 mice were used as controls. Data are presented as mean ± SE. (C) Brain sections from Tg2576 or C57BL/6 mice were examined for Aß deposits by immunohistostaining using rabbit anti-human beta amyloid 1–42 polyclonal antibody.
doi:10.1371/journal.pone.0057606.g006

Recent reports suggest that mAb therapy is effective only in AD patients possessing e4/c4 proteins [12,41]. In this context, ApoE4 (+) individuals develop AD more often than ApoE4 (−) individuals [42–43]. Such observations help inform the design of trials with AAV vectors intended for human use, as it facilitates the identification of individuals at high risk for developing AD. In addition, previous studies documented that Aß oligomers are toxic to neuronal cells [44–45]. That finding is consistent with current results showing that aggregated Aß proteins are toxic to primary culture neuronal cells and that anti-Aß mAbs prevent this toxicity (Figure 3).

We hypothesize that the ongoing accumulation of Aß aggregates is responsible for widespread neuronal cell degeneration and the subsequent dementia characteristic of AD. We believe that the failure of clinical trials involving anti-Aß mAb may reflect
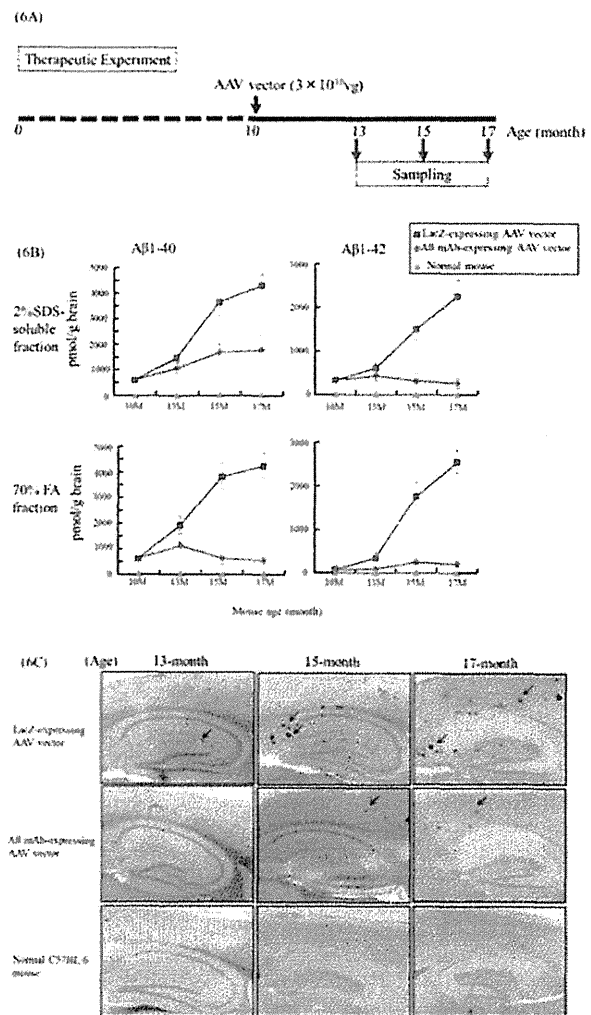
the late initiation of such treatment as it is important to eliminate Aß oligomers during the early stages of AD. Evidence that ApoE4 and other factors can predict individuals at high risk [34] lead us to recommend clinical trials of Aß mAb - expressing AAV vector commence at an early age for prophylaxis of AD. Current results show that the production of anti-Aß mAbs persists for an extended period (Figure 4). Thus, a single early treatment may yield long term clinical benefit. Further study that includes behavioral and memory testing combined with even longer follow should help clarify the value of AAV vector mediated in the prophylaxis and/ or therapy of AD treatment.

Taken together, we constructed an anti-Aβ Ab-expressing AAV vector. A single intramuscular injection of the vector generated high serum anti-Aß Ab level for up to 64 weeks, and significantly

−311−

decreased Aß levels in the brain of AD model mice treated at 5 months (prophylactic) or 10 months (therapeutic) of age. Our present results clearly demonstrated that the Aß mAb-expressing AAV vector may be of prophylactic and/or therapeutic value for AD treatment.

Materials and Methods

Ethics Statement

All animal work has been conducted according to relevant Japan and international guidelines. All experimental procedures were carried out in accordance with the Administrative Panel on Laboratory Animal Care (APLAC) protocol and the institutional guidelines set by Yokohama City University and Chyoju Medical Institute. The protocols used in this study were proved by Institutional Animal Care and Use Committee (IACUC)/Ethics committee of Yokohama City University (No. 0741, 0875 and 0974) and Chyoju Medical Institute (No. B-22).

All animal work has been conducted according to relevant U.S. and international guidelines. Specifically, all experimental procedures were carried out in accordance with the Administrative Panel on Laboratory Animal Care (APLAC) protocol and the institutional guidelines set by the Veterinary Service Center at Stanford University (Animal Welfare Assurance A3213-01 and USDA License 93-4R-00). Stanford APLAC and institutional guidelines are in compliance with the U.S. Public Health Service Policy on Humane Care and Use of Laboratory Animals. The Stanford APLAC approved the animal protocol associated with the work described in this publication.

Genes of mAbs against Aß

A hybridoma producing anti-Aß1–13 mAb (IIA2) [14] was cultured in KBM 450 medium (Kohjin Bio Co., Ltd., Saitama, Japan) in the absence of fetal bovine serum (FBS). The antibody was concentrated and partially purified from culture supernatant by ammonium sulfate precipitation and was used for the experiments as a positive control.

Aß peptide synthesis and aggregated Aß or oligomer formation

The Aß1-42 peptide used in these studies was produced by chemical synthesis (American Peptide, Sunnyvale, CA, USA). Reverse - phase high performance liquid chromatography showed that the synthesized peptide has >95% purity, and mass spectrometry analysis verified the molecular mass. Oligomer formation was done using the method described previously (Stine et al., 2003). Briefly, Aß oligomers were prepared by diluting 5 mM Aß1–42 in Me2SO to 100 µM in ice-cold cell culture supernatant (phenol red - free Ham's F-12; BioSource, CA, USA), immediately vortexing for 30 s, and incubating at 4°C, room temperature or 37°C for 24 h. The aggregated Aß or oligomer solution was used for the Western blotting analysis, as well as cytotoxic tests of neural cells.

Construction of an expression vector for the anti-Aß mAb gene

Total RNA was extracted from a hybridoma producing anti-Aß1–13 mAb (IIA2) [14] using TRIzol Reagent (Gibco BRL, Grand Island, NY, USA). Full-length heavy (H) chain and light (L) chain cDNA was transcribed with 5'-RACE primer and 3'-RACE primer using BD SMART RACE cDNA Amplification Kit (Clontech, Mountain View, CA, USA) according to the manufacturer's instructions. H chain cDNA was amplified with sense primer (5' CGG GGT ACC ATG GGC AGG CTT ACT TCT TC 3') and antisense primer (5' CCC AAG CTT TTT ACC AGG AGA GTG GGA GA 3'). L chain cDNA was amplified with sense primer (5' CCG GAA TTC ATG GAG ACA GAC ACA CTC CT 3') and antisense primer (5' ATA AGA ATG CGG CCG CA G TCG ACG CTA ACA CTC ATT CCT GTT GA 3'). The Furin 2A fragment [46–47] from the foot and mouth disease virus was synthesized with complementary oligo (5' CCC AAG CTT CGC GCC AAG CGC GCC CCC GT 3' and 5' CCG GAA TTC GGG GCC GGG GTT GGA CTC CA 3'). The H chain–Furin 2A–L chain fusion fragment was subcloned into proviral plasmid pW1 controlled by the CMV promoter. The AAV vectors were prepared by the previously described three - plasmid transfection adenovirus-free protocol [16,48]. Briefly, 60% confluent human embryonic kidney 293 (HEK293) cells were maintained in Dulbecco's modified Eagle's medium – nutrient mixture F-12 (1:1) (DMEM/F-12; GIBCOBRL, New York, NY) supplemented with 10% fetal bovine serum (FBS). Cells were cultured at 37°C in an atmosphere of 5% CO_2 in air. Subconfluent HEK293 cells were co-transfected by the calcium phosphate co-precipitation method with the AAV shuttle plasmid pW1 (containing LacZ or antibody heavy chain-F2A-light chain), the AAV-1 chimeric helper plasmid p1RepCap (provided by Dr. James M. Wilson, University of Pennsylvania, Philadelphia, PA, USA), and the adenoviral helper plasmid pAdeno (provided by Avigen, Inc., Alamada, CA, USA). After 48 h, the cells were harvested and lysed in Tris buffer (10 mM Tris-HCl, 150 mM NaCl, pH 8.0) by three cycles of freezing and thawing. One round of sucrose precipitation and two rounds of CsCl density-gradient ultracentrifugation were sufficient to isolate the AAV vector from the lysates. The vector titer was determined by quantitative PCR and presented as vg.

Western blot analysis

To confirm the expression of the Ab proteins, HEK293 cells were transduced with the AAV vector encoding the mAb genes (Aß mAb-expressing vector) in a 6-well plate. After transduction of AAV vector for 2 h, the cells were washed twice with PBS and cultured with Ex-CELL CD CHO serum-free medium (Life Technologies Japan Ltd, Tokyo, Japan) for another 2 days. Then, antibody protein was detected in culture supernatant and cell lysates with Western blot. The cells were washed with PBS and lysed with 0.1 M Tris-HCl (pH 7.8) and 0.125% Nonidet P-40 2 days after transduction. The cell lysates were mixed with an equal volume of 2× SDS buffer (125 mM Tris-HCl [pH 6.8], 4% SDS) with 100 mM of DTT (reducing condition) or without DTT (non-reducing condition) and boiled for 10 min. The cell lysates were loaded on an 8% polyacrylamide gel and transferred to a Hybond ECL nitrocellulose membrane. After rinsing with PBS, the membrane was probed with HRP-labeled goat anti-mouse IgG1 or IgκAbs (Ig; ICN Pharmaceuticals Inc., Solon, OH, USA). The protein was detected using the ECL Plus Western Blotting Detection System (Amersham Pharmacia Biotech, Uppsala, Sweden).

Animals and administration

Heterozygous Tg2576 mice were obtained from Taconic Farms Inc. (Germantown, NY, USA) [14]. Normal C57BL/6 female mice were purchased from Japan SLC Inc. (Hamamatsu, Japan). The mice were housed in the animal centers located at Yokohama City University and Chyoju Medical Institute, and maintained on a 12-h day–night cycle. Five-month and 10-month old mice were used for prophylactic and therapeutic experiments, respectively. The mice were received a single injection in quadriceps muscles

—312—

with a dose of 3.0×10^{10} vg of the Aß mAb-expressing vector. We used 20–25 mice in each group. The mice for prophylactic experiments were sacrificed 5, 8, 10 and 12 months after Aß mAb - expressing vector administration and the mice for therapeutic experiments were sacrificed 0, 3, 5 and 7 months after Aß mAb-expressing vector administration. To explore the magnitude and duration of antibody expression, we injected 3.0×10^9, 3.0×10^{10} and 3.0×10^{11} vg of Aß mAb-expressing vector or 3.0×10^{11} vg of AAV vector expressing LacZ gene (LacZ-expressing vector) to mouse quadriceps muscles, and blood was collected at indicated time points for Aß-specific antibody detection. The animal experiments were approved by the Animal Ethical Committees of Yokohama City University School of Medicine and and Chyoju Medical Institute.

Enzyme-linked immunosorbent assay (ELISA) for Ab titers

ELISA was performed as described previously [14]. Briefly, 96-well microtiter plates were coated with 40 µg/ml of Aß1-42 peptide in 0.15 M phosphate-buffered saline (PBS). The wells were rinsed with 0.15 M PBS and then blocked with 3% FBS in 0.15 M PBS for 1 h. Appropriately diluted mAb as well as the serum from AAV vector-administered mouse were incubated on antigen-coated plates for 6 h at 4°C. Then, wells were rinsed with 0.15 M PBS and the bound Abs were detected using HRP-coupled goat anti-mouse IgG1 (Pierce Chemical Co., Rockford, IL, USA). We detected IgG1 titer rather than total IgG titer, because transgene of the AAV vector was isolated from the mouse IgG1-secreting hybridoma (IIA2). The anti-Aß1–13 mAb (IIA2) purified from the hybridoma was used as a standard control.

Brain sample preparation for histochemical studies

Brains were removed and divided sagittally along the interhemispheric fissure. The right hemisphere was dissected from the cerebella. Brain samples were snap frozen in large test tubes containing n-hexane, immersed in a dry ice/acetone mixture, and stored at −80°C until processing. The left hemisphere was fixed with formalin and then embedded in paraffin for histochemical studies. To test whether Aß mAb-expressing vector-produced antibody can be used for immunostaining against human Aß, Culture supernatant of Aß mAb - expressing vector-transduced HEK293 cells was used as a first antibody and HRP-Goat anti-mouse IgG1 antibody used as a second antibody. Rabbit anti-human beta amyloid (1–42) antibody (Genetex, Inc., Irvine, CA) and mAb purified from hybridoma IIA2 were used as controls. Paraffin samples from AAV vector administrated mice were stained with the rabbit anti-human beta amyloid (1–42) antibody.

ELISA to measure Aß protein levels in the brain

The frozen left cerebra were obtained from each mouse and homogenized with a homogenizer in Tris-buffered saline buffer (TBS, 50 mM Tris, 150 mM NaCl, pH 7.6) containing protease inhibitor cocktail (Nacalai, San Diego, CA, USA) with 20 µg/ml pepstatin A, then centrifuged at 100,000 g for 1 h at 4°C using an Optima TLX ultracentrifuge (Beckman Coulter Inc., Fullerton, CA, USA). The pellets were homogenized in TBS buffer containing 2% SDS and protease inhibitor cocktail (Nacalai, San

Diego, CA, USA) following incubation at 37°C for 15 min. Then the solution was centrifuged again at 100,000 g for 1 h at 25°C. The supernatant and pellet correspond to the soluble (2% SDS soluble fraction) and insoluble fraction, respectively.

The insoluble fraction was washed, then extracted again with 70% formic acid and centrifuged at 100,000 g for 1 h. The supernatants of 70% formic acid extracts were neutralized with 1 M Tris-HCl, pH 8.0 at a dilution of 1:20 (70% FA fraction). The dissolved samples of Aß1–42 or Aß1–40 protein were quantified using Human Amyloid ß (N3pE-42) Kit and Human Amyloid ß (N3pE-40) assay kit, respectively (IBL Co., Ltd., Gunma, Japan). The values obtained were corrected with the wet weight of each brain hemisphere sample and expressed as pmol/g brain.

Cytotoxicity inhibition test by Abs from AAV-transduced cells using primary culture hippocampal cell

Hippocampal cells were collected from 15-day-old fetal mouse brains and gently minced. The samples were incubated at 37°C for 5 min in 9 ml of 0.15 M PBS and 1 ml of 2.5% trypsin, followed by addition of 1 ml 0.5% trypsin inhibitor on ice. The cells were washed twice with 0.15 M PBS and resuspended in media stock (MS) supplemented with 20% FBS, 10 ng/ml epidermal growth factor, 50 IU/ml penicillin, and 50 µg/mL streptomycin. MS is composed of modified Eagle's medium supplemented with 2 mM glutamine and 20 mM glucose [49].

We reacted 5.0×10^4 primary culture hippocampal cells in 100 µl MS per well with each concentration of aggregated Aß solution with or without Aß mAb - expressing vector-transduced culture supernatant in a humidified atmosphere (37°C, 5% CO2). After 6 and 24 h incubation, 10 µL 3-[4,5-dimethylthiazol-2-yl]-2,5-diphenyl tetrazolium bromide (MTT) reagent (final concentration 0.5 mg/ml) was added to each well. The microplate was incubated for 4 h in a humidified atmosphere [50]. Then, 100 µl of the solubilization solution was added into each well to solubilize the purple formazan crystals, and the absorbance of the samples was measured using an ELISA microplate reader [51].

Data analysis

All values were expressed as the mean ± standard error (SE). Statistical analysis (Student's t-test) of the experimental data and controls was conducted using two-way factorial analysis of variance. Significance was defined as $P < 0.05$ for statistical analysis using all time points in each group.

Acknowledgments

Author Contributions

Conceived and designed the experiments: K. Ozawa K. Okuda. Performed the experiments: MS SA TT. Analyzed the data: KS DMK. Contributed reagents/materials/analysis tools: MO HM. Wrote the paper: MS K. Okuda.

References

1. De Felice FG, Wu D, Lambert MP, Fernandez SJ, Velasco PT, et al. (2008) Alzheimer's disease-type neuronal tau hyperphosphorylation induced by A beta oligomers. Neurobiol Aging. 29: 1334–1347.

2. Zhang YW, Thompson R, Zhang H, Xu H (2011) APP processing in Alzheimer's disease. Mol Brain. 4: 3.

3. Schenk D, Barbour R, Dunn W, Gordon G, Grajeda H, et al. (1999) Immunization with amyloid-beta attenuates Alzheimer-disease-like pathology in the PDAPP mouse. Nature. 400: 173–177.

4. Morgan D, Diamond DM, Gottschall PE, Ugen KE, Dickey C, et al. (2000) A beta peptide vaccination prevents memory loss in an animal model of Alzheimer's disease. Nature. 408: 982–985.

−313−

5. Nicoll JA, Wilkinson D, Holmes C, Steart P, Markham H, et al. (2003) Neuropathology of human Alzheimer disease after immunization with amyloid-beta peptide: a case report. Nat Med. 9: 448–452.

6. Ferrer I, Boada Rovira M, Sanchez Guerra ML, Rey MJ, Costa-Jussa F (2004) Neuropathology and pathogenesis of encephalitis following amyloid-beta immunization in Alzheimer's disease. Brain Pathol. 14: 11–20.

7. Check E (2002) Nerve inflammation halts trial for Alzheimer's drug. Nature. 415: 462.

8. Orgogozo JM, Gilman S, Dartigues JF, Laurent B, Puel M, et al. (2003) Subacute meningoencephalitis in a subset of patients with AD after Abeta42 immunization. Neurology. 61: 46–54.

9. Nicoll JA, Barton E, Boche D, Neal JW, Ferrer I, et al. (2006) Abeta species removal after abeta42 immunization. J Neuropathol Exp Neurol. 65: 1040–1048.

10. Holmes C, Boche D, Wilkinson D, Yadegarfar G, Hopkins V, et al. (2008) Long-term effects of Abeta42 immunisation in Alzheimer's disease: follow-up of a randomised, placebo-controlled phase I trial. Lancet. 372: 216–223.

11. DeMattos RB, Bales KR, Cummins DJ, Dodart JC, Paul SM, et al. (2001) Peripheral anti-A beta antibody alters CNS and plasma A beta clearance and decreases brain A beta burden in a mouse model of Alzheimer's disease. Proc Natl Acad Sci U S A. 98: 8850–8855.

12. Salloway S, Sperling R, Gilman S, Fox NC, Blennow K, et al. (2009) A phase 2 multiple ascending dose trial of bapineuzumab in mild to moderate Alzheimer disease. Neurology. 73: 2061–2070.

13. Black RS, Sperling RA, Safirstein B, Motter RN, Pallay A, et al. (2010) A single ascending dose study of bapineuzumab in patients with Alzheimer disease. Alzheimer Dis Assoc Disord. 24: 198–203.

14. Tamura Y, Hamajima K, Matsui K, Yanoma S, Narita M, et al. (2005) The F(ab)'2 fragment of an Abeta-specific monoclonal antibody reduces Abeta deposits in the brain. Neurobiol Dis. 20: 541–549.

15. Pfeifer M, Boncristiano S, Bondolfi L, Stalder A, Deller T, et al. (2002) Cerebral hemorrhage after passive anti-Abeta immunotherapy. Science. 298: 1379.

16. Xin KQ, Urabe M, Yang J, Nomiyama K, Mizukami H, et al. (2001) A novel recombinant adeno-associated virus vaccine induces a long-term humoral immune response to human immunodeficiency virus. Hum Gene Ther. 12: 1047–1061.

17. Stine WB Jr, Dahlgren KN, Krafft GA, LaDu MJ (2003) In vitro characterization of conditions for amyloid-beta peptide oligomerization and fibrillogenesis. J Biol Chem. 278: 11612–11622.

18. Brantly ML, Spencer LT, Humphries M, Conlon TJ, Spencer CT, et al. (2006) Phase I trial of intramuscular injection of a recombinant adeno-associated virus serotype 2 alpha1-antitrypsin (AAT) vector in AAT-deficient adults. Hum Gene Ther. 17: 1177–1186.

19. Jiang H, Pierce GF, Ozelo MC, de Paula EV, Vargas JA, et al. (2006) Evidence of multiyear factor IX expression by AAV-mediated gene transfer to skeletal muscle in an individual with severe hemophilia B. Mol Ther. 14: 452–455.

20. Hara H, Monsonego A, Yuasa K, Adachi K, Xiao X, et al. (2004) Development of a safe oral Abeta vaccine using recombinant adeno-associated virus vector for Alzheimer's disease. J Alzheimers Dis. 6: 483–488.

21. Mouri A, Noda Y, Hara H, Mizoguchi H, Tabira T, et al. (2007) Oral vaccination with a viral vector containing Abeta cDNA attenuates age-related Abeta accumulation and memory deficits without causing inflammation in a mouse Alzheimer model. FASEB J. 21: 2135–2148.

22. Fukuchi K, Tahara K, Kim HD, Maxwell JA, Lewis TL, et al. (2006) Anti-Abeta single-chain antibody delivery via adeno-associated virus for treatment of Alzheimer's disease. Neurobiol Dis. 23: 502–511.

23. Levites Y, Jansen K, Smithson LA, Dakin R, Holloway VM, et al. (2006) Intracranial adeno-associated virus-mediated delivery of anti-pan amyloid beta, amyloid beta40, and amyloid beta42 single-chain variable fragments attenuates plaque pathology in amyloid precursor protein mice. J Neurosci. 26: 11923–11928.

24. Sudol KL, Mastrangelo MA, Narrow WC, Frazer ME, Levites YR, et al. (2009) Generating differentially targeted amyloid-beta specific intrabodies as a passive vaccination strategy for Alzheimer's disease. Mol Ther. 17: 2031–2040.

25. Ryan DA, Mastrangelo MA, Narrow WC, Sullivan MA, Federoff HJ, et al. (2010) Abeta-directed single-chain antibody delivery via a serotype-1 AAV vector improves learning behavior and pathology in Alzheimer's disease mice. Mol Ther. 18: 1471–1481.

26. Kou J, Kim H, Pattanayak A, Song M, Lim JE, et al. (2011) Anti-Amyloid-beta Single-Chain Antibody Brain Delivery Via AAV Reduces Amyloid Load But May Increase Cerebral Hemorrhages in an Alzheimer's Disease Mouse Model. J Alzheimers Dis. 27: 23–38.

27. Feng X, Eide FF, Jiang H, Reder AT (2004) Adeno-associated viral vector-mediated ApoE expression in Alzheimer's disease mice: low CNS immune response, long-term expression, and astrocyte specificity. Front Biosci. 9: 1540–1546.

28. Carty NC, Nash K, Lee D, Mercer M, Gottschall PE, et al. (2008) Adeno-associated viral (AAV) serotype 5 vector mediated gene delivery of endothelin-converting enzyme reduces Abeta deposits in APP + PS1 transgenic mice. Mol Ther. 16: 1580–1586.

29. Liu Y, Studzinski C, Beckett T, Guan H, Hersh MA, et al. (2009) Expression of neprilysin in skeletal muscle reduces amyloid burden in a transgenic mouse model of Alzheimer disease. Mol Ther. 17: 1381–1386.

30. Mandel RJ (2010) CERE-110, an adeno-associated virus-based gene delivery vector expressing human nerve growth factor for the treatment of Alzheimer's disease. Curr Opin Mol Ther. 12: 240–247.

31. Chu J, Giannopoulos PF, Ceballos-Diaz C, Golde TE, Pratico D (2012) Adeno-associated virus-mediated brain delivery of 5-lipoxygenase modulates the AD-like phenotype of APP mice. Mol Neurodegener. 7: 1.

32. Fitch JC, Rollins S, Matis L, Alford B, Aranki S, et al. (1999) Pharmacology and biological efficacy of a recombinant, humanized, single-chain antibody C5 complement inhibitor in patients undergoing coronary artery bypass graft surgery with cardiopulmonary bypass. Circulation. 100: 2499–2506.

33. Bard F, Cannon C, Barbour R, Burke RL, Games D, et al. (2000) Peripherally administered antibodies against amyloid beta-peptide enter the central nervous system and reduce pathology in a mouse model of Alzheimer disease. Nat Med. 6: 916–919.

34. McCarron MO, Nicoll JA (2004) Cerebral amyloid angiopathy and thrombo-lysis-related intracerebral haemorrhage. Lancet Neurol. 3: 484–492.

35. Schroeter S, Khan K, Barbour R, Doan M, Chen M, et al. (2008) Immunotherapy reduces vascular amyloid-beta in PDAPP mice. J Neurosci. 28: 6787–6793.

36. Wilcock DM, Alamed J, Gottschall PE, Grimm J, Rosenthal A, et al. (2006) Deglycosylated anti-amyloid-beta antibodies eliminate cognitive deficits and reduce parenchymal amyloid with minimal vascular consequences in aged amyloid precursor protein transgenic mice. J Neurosci. 26: 5340–5346.

37. Karlnoski RA, Rosenthal A, Alamed J, Ronan V, Gordon MN, et al. (2008) Deglycosylated anti-Abeta antibody dose-response effects on pathology and memory in APP transgenic mice. J Neuroimmune Pharmacol. 3: 187–197.

38. Chackerian B, Rangel M, Hunter Z, Peabody DS (2006) Virus and virus-like particle-based immunogens for Alzheimer's disease induce antibody responses against amyloid-beta without concomitant T cell responses. Vaccine. 24: 6321–6331.

39. Nikolic WV, Bai Y, Obregon D, Hou H, Mori T, et al. (2007) Transcutaneous beta-amyloid immunization reduces cerebral beta-amyloid deposits without T cell infiltration and microhemorrhage. Proc Natl Acad Sci U S A. 104: 2507–2512.

40. Okura Y, Miyakoshi A, Kohyama K, Park IK, Staufenbiel M, et al. (2006) Nonviral Abeta DNA vaccine therapy against Alzheimer's disease: long-term effects and safety. Proc Natl Acad Sci U S A. 103: 9619–9624.

41. Farlow MR (2010) Should the ApoE genotype be a covariate for clinical trials in Alzheimer disease? Alzheimers Res Ther. 2: 15.

42. Dafnis I, Stratikos E, Tzinia A, Tsilibary EC, Zannis VI, et al. (2010) An apolipoprotein E4 fragment can promote intracellular accumulation of amyloid peptide beta 42. J Neurochem. 115: 873–884.

43. Fleisher AS, Chen K, Liu X, Ayutyanont N, Roontiva A, et al. (2012) Apolipoprotein E epsilon4 and age effects on florbetapir positron emission tomography in healthy aging and Alzheimer disease. Neurobiol Aging.

44. Yankner BA, Duffy LK, Kirschner DA (1990) Neurotrophic and neurotoxic effects of amyloid beta protein: reversal by tachykinin neuropeptides. Science. 250: 279–282.

45. Takuma H, Teraoka R, Mori H, Tomiyama T (2008) Amyloid-beta E22Delta variant induces synaptic alteration in mouse hippocampal slices. Neuroreport. 19: 615–619.

46. Fang J, Qian JJ, Yi S, Harding TC, Tu GH, et al. (2005) Stable antibody expression at therapeutic levels using the 2A peptide. Nat Biotechnol. 23: 584–590.

47. Shoji M, Yoshizaki S, Mizuguchi H, Okuda K, Shimada M (2012) Immunogenic comparison of chimeric adenovirus 5/35 vector carrying optimized human immunodeficiency virus clade C genes and various promoters. PLoS One. 7: e30302.

48. Okada T, Nomoto T, Yoshioka T, Nonaka-Sarukawa M, Ito T, et al. (2005) Large-scale production of recombinant viruses by use of a large culture vessel with active gassing. Hum Gene Ther. 16: 1212–1218.

49. Akiyama H, Mori H, Saido T, Kondo H, Ikeda K, et al. (1999) Occurrence of the diffuse amyloid beta-protein (Abeta) deposits with numerous Abeta-containing glial cells in the cerebral cortex of patients with Alzheimer's disease. Glia. 25: 324–331.

50. Berridge MV, Herst PM, Tan AS (2005) Tetrazolium dyes as tools in cell biology: new insights into their cellular reduction. Biotechnol Annu Rev. 11: 127–152.

51. Hsiao K, Chapman P, Nilsen S, Eckman C, Harigaya Y, et al. (1996) Correlative memory deficits, Abeta elevation, and amyloid plaques in transgenic mice. Science. 274: 99–102.

—314—

ORIGINAL ARTICLE

Anti-factor IXa/X bispecific antibody (ACE910): hemostatic potency against ongoing bleeds in a hemophilia A model and the possibility of routine supplementation

A. MUTO,* K. YOSHIHASHI,* M. TAKEDA,* T. KITAZAWA,* T. SOEDA,* T. IGAWA,*
Y. SAKAMOTO,* K. HARAYA,* Y. KAWABE,* M. SHIMA,† A. YOSHIOKA‡ and K. HATTORI*

*Research Division, Chugai Pharmaceutical Co., Ltd, Gotemba, Shizuoka; †Department of Pediatrics, Nara Medical University; and ‡Nara Medical University, Kashihara, Nara, Japan

Summary. *Background:* We previously reported that a humanized anti-factor IXa/X bispecific antibody, hBS23, mimics the function of FVIII even in the presence of FVIII inhibitors, and has preventive hemostatic activity against bleeding in an animal model of acquired hemophilia A. After further molecular engineering of hBS23, we recently identified an improved humanized bispecific antibody, ACE910, for clinical investigation. *Objectives:* To elucidate the *in vivo* hemostatic potency of ACE910 by examining its effect against ongoing bleeds, and to determine its pharmacokinetic parameters for discussion of its potency for prophylactic use. *Methods:* A non-human primate model of acquired hemophilia A was established by injecting anti-primate FVIII neutralizing antibody. When bleeds emerged following an artificial bleed-inducing procedure, either ACE910 or recombinant porcine FVIII (rpoFVIII) was intravenously administered. rpoFVIII was additionally administered twice daily on the following 2 days. Bleeding symptoms were monitored for 3 days. A pharmacokinetic study and multiple-dosing simulations of ACE910 were also performed. *Results:* A single bolus of 1 or 3 mg kg^{-1} ACE910 showed hemostatic activity comparable to that of 10 U kg^{-1} (twice daily) rpoFVIII against ongoing bleeds. The determined ACE910 pharmacokinetic parameters included a long half-life (3 weeks) and high subcutaneous bioavailability (nearly 100%). The simulation results based on pharmacokinetic parameters indicated that the above hemostatic level could be maintained with once-weekly subcutaneous administration of ACE910, suggesting the possibility of more effective prophylaxis. *Conclusions:* ACE910 may offer an alternative on-demand treatment option for patients with hemophilia A, as well as user-friendly and aggressive routine supplementation.

Keywords: antibodies, catalytic; factor VIII; hemophilia A; hemostasis; therapeutics.

Correspondence: Atsushi Muto, Research Division, Chugai Pharmaceutical Co., Ltd, 1-135 Komakado, Gotemba, Shizuoka 412-8513, Japan.
Tel.: +81 550 87 3411; fax: +81 550 87 1960.
E-mail: mutoats@chugai-pharm.co.jp

Institution where the work was carried out: Research Division, Chugai Pharmaceutical Co., Ltd.

Introduction

Hemophilia A is a bleeding disorder caused by an inherited deficiency of factor VIII. The severity is known to correlate with the plasma FVIII level: severe, moderate and mild phenotypes are defined by plasma FVIII levels of < 1, 1–5 and > 5 to < 40 U dL^{-1}, respectively. Severe cases have a high propensity to suffer bleeds, including joint bleeds, whereas moderate cases typically experience far fewer bleeding episodes, and mild cases rarely bleed spontaneously [1,2].

Patients are primarily treated with FVIII agents. However, as FVIII agents are exogenous for severely affected patients, ~ 30% of them develop alloantibodies against FVIII (FVIII inhibitors) [2]. FVIII inhibitors largely restrict treatment with FVIII agents, and consequently make it difficult to control bleeding, because alternative bypassing agents have shorter *in vivo* half-lives and are not always effective [3]. The eradication of FVIII inhibitors with high doses of FVIII is very expensive, and does not always work [4]. In patients with severe hemophilia A without FVIII inhibitors, routine prophylaxis with exoge-

nous FVIII to maintain FVIII levels above 1 U dL^{-1} is beneficial to prevent bleeding [5,6]; however, the need for frequent intravenous injections negatively affects patients' quality of life [7].

In order to overcome these shortcomings, we previously created a humanized anti-FIXa/FX bispecific IgG antibody, termed hBS23, which replicated FVIII cofactor function by binding and placing FIXa and FX into spatially appropriate positions [8]. hBS23 had cofactor activity *in vitro*, even in the presence of FVIII inhibitors, and, in a non-human primate model of acquired hemophilia A, hBS23 at an intravenous dose of 0.3 mg kg^{-1} exerted hemostatic activity to prevent the progression of bleeding symptoms to the same extent as recombinant porcine FVIII (rpoFVIII) maintained at a plasma level of $\geq$ 1 U dL^{-1}. However, it remained unproven whether this bispecific antibody approach possessed the potency to ameliorate ongoing bleeds, which would require higher levels of FVIII, or how much hemostatic potency it had in comparison with FVIII. We recently modified hBS23 with a multidimensional optimization approach to improve the FVIII-mimetic cofactor activity, pharmacokinetic properties, immunogenicity, physicochemical stability, and ease of industrial manufacture for clinical application; we consequently identified an improved humanized anti-FIXa/FX bispecific IgG antibody, termed ACE910 [9]. In this study, we elucidate the *in vivo* hemostatic potency of ACE910, including that against ongoing bleeds as compared with rpoFVIII, by using a non-human primate model of acquired hemophilia A.

Furthermore, in order to elucidate the potency of ACE910 in routine supplementation, we performed a pharmacokinetic study of ACE910 in non-human primates to determine its pharmacokinetic parameters, and conducted multiple dosing simulations with those parameters. Routine supplementation with exogenous FVIII is aimed at keeping the FVIII level at 1 U dL^{-1} or above to convert a severe disease to a moderate one [2,5]. This strategy successfully reduces bleeding episodes and the risk of developing hemophilic arthropathy [5]. However, the effect is not necessarily perfect: a recent report suggested that the risk of joint damage remains until the baseline factor level is 10–15 U dL^{-1} or higher [10]. In this study, we also discuss the possibility of once-weekly subcutaneous administration of ACE910 for routine supplementation that is more aggressive than the current one with exogenous FVIII; in other words, a regimen that can convert a severe disease to a mild disease.

Materials and methods

Materials

ACE910 was expressed in human embryonic kidney 293 or Chinese hamster ovary (CHO) cells, which were co-transfected with the mixture of plasmids encoding the humanized anti-FIXa heavy chain, anti-FX heavy chain, and common light chain. ACE910 was purified by protein A and ion exchange chromatography from the culture supernatant [9]. B domain-deleted rpoFVIII [8] was prepared as described in the supporting information (Preparation and analysis of rpoFVIII). Briefly, we expressed it in CHO cells by stable transfection. Then, rpoFVIII was purified from the supernatant by using ion exchange and gel permeation chromatography. We confirmed its purity with SDS-PAGE under reduced conditions, and determined its activity (U dL^{-1}) with an activated partial thromboplastin time (APTT)-based one-stage coagulation assay. Recombinant human FVIII (rhFVIII) was purchased from Bayer HealthCare (Leverkusen, Germany). Anti-primate FVIII neutralizing antibody (VIII-2236) [8] and the other purchased reagents are described in the supporting information (Confirmation of non-reactivity of VIII-2236 to rpoFVIII and ACE910, and the other supporting methods).

Animals and ethics

We used 26 and 12 male cynomolgus monkeys for the *in vivo* hemostatic study (2.6–4.0 kg, aged 3 years; Hamri, Ibaraki, Japan) and for the pharmacokinetic study (2.9–5.0 kg, aged 4–5 years; Japan Laboratory Animals, Tokyo, Japan), respectively. We used 24 female mice (aged 5 weeks; Charles River, Yokohama, Japan, and SLC, Hamamatsu, Japan) and 24 female rats (aged 4 weeks; Charles River) for the immunization to generate anti-idiotype antibodies against the variable region of ACE910. The details of anti-idiotype antibodies are described in the supporting information (Generation and preparation of anti-idiotype antibodies to each variable region of ACE910).

All animal studies were approved by the Institutional Animal Care and Use Committee of Chugai Pharmaceutical, and were conducted in accordance with the approved protocols and the Guidelines for the Care and Use of Laboratory Animals at the company. Chugai Pharmaceutical is fully accredited by the Association for Assessment and Accreditation of Laboratory Animal Care International.

APTT and thrombin generation (TG) assays

APTT and TG assays were performed with standard equipment. In the TG assay, we employed two kinds of triggering solutions that contained, respectively, FXIa and tissue factor (TF). The solution containing human FXIa (Enzyme Research Laboratories, Swansea, UK) was prepared in-house, and the solution containing TF, PPP-Reagent LOW (Thrombinoscope BV, Maastricht, the Netherlands) was purchased. The details are described in the supporting information (APTT and TG assays).

In vivo hemostatic study in an acquired hemophilia A model

As ACE910 is highly species-specific in its FVIII-mimetic cofactor activity, non-human primates were used. On day 0, the animals received an intravenous injection of VIII-2236 (10 mg kg^{-1}). Two hours later, the animals were anesthetized with isoflurane inhalation, and bruises on the body surface that might possibly have emerged because of FVIII neutralization were measured. Then, the following two surgical procedures were performed: a 18G-needle was inserted 1 cm deep into the muscle at 22 sites (two sites in each upper arm, three sites in each forearm, four sites on the inside of each thigh, and two sites on the outside of each thigh); and subcutaneous exfoliation was performed by inserting the tip of forceps beneath the abdominal skin to 3 cm at two sites. After administration of buprenorphine, an analgesic drug, the animals were allowed to recover from the anesthesia. (They received this analgesic treatment twice daily [morning and evening] from day 0 to day 2; six doses were given, and the condition of the animals was observed daily.) After recognition of bleeding, approximately 6–8 h after injury, the animals received intravenous ACE910 (0.3, 1 or 3 mg kg^{-1}; $n = 4$ for each group), rpoFVIII (3.4 or 10 U kg^{-1}; $n = 4$ for each group), or no test item (control; $n = 6$). In the rpoFVIII group, rpoFVIII was also intravenously administered in the morning and evening on days 1 and 2 (a total of five administrations). In the morning on days 1, 2, and 3, the animals were anesthetized for measurement of the bruised areas. After the evaluation on day 3, the animals were killed humanely. Citrated blood was collected before and 2 h after the VIII-2236 injection, ~ 10 min after the test item administration on day 0, and before measurement of the bruised area on days 1, 2, and 3. The change in blood hemoglobin level was expressed as a percentage of that on day 0 (2 h after the VIII-2236 injection). The plasma ACE910 concentration was determined with the method described in the supporting information (Measurement of plasma ACE910 concentration).

Pharmacokinetic study

Animals received intravenous ACE910 (6 mg kg^{-1}; $n = 3$) or subcutaneous ACE910 (0.06, 0.6 or 6 mg kg^{-1}; $n = 3$ for each group) in a single dose. For animals dosed intravenously, blood was sampled with a heparinized syringe at 0.25, 2, 8, 24, 48, 72 and 96 h postdose, as well as at 7, 14, 28, 42, 56, 70 and 84 days postdose. For animals dosed subcutaneously, blood was collected in the same way without sampling at 0.25 h. The plasma concentrations of ACE910 and anti-ACE910 alloantibodies were measured with the methods described in the supporting information (Measurement of plasma ACE910 concentration and detection of anti-ACE910 alloantibodies).

Statistical analysis, pharmacokinetic analysis, and multiple-dosing simulation

For the *in vivo* hemostatic study, data are presented as mean ± standard error. Other data are presented as mean ± standard deviation. The parametric Dunnett multiple comparison test (two-tailed) (SAS preclinical package version 5.00; SAS Institute Japan, Tokyo, Japan) was used to determine *P*-values. $P < 0.05$ was considered to be statistically significant.

In the pharmacokinetic study, the plasma ACE910 concentration data were analyzed by non-compartmental analysis with PHOENIX WINNONLIN version 6.2 (Pharsight, St Louis, MO, USA). Multiple-dosing simulations were performed with SAAM II version 1.2 (SAAM Institute, Seattle, WA, USA).

Results

In vitro cross-reactivity of ACE910 with cynomolgus monkeys

First, we examined the cross-reactivity of ACE910 with cynomolgus monkeys by use of an APTT assay. ACE910 shortened APTT in FVIII-neutralized cynomolgus monkey plasma with a concentration dependency similar to that in human FVIII-deficient plasma (Fig. 1A,B).

We next examined the cross-reactivity of ACE910 with cynomolgus monkeys by use of one of the global assays, the TG assay [11]. Because we had not clearly detected rpoFVIII activity in the standard low-TF triggering condition in FVIII-neutralized cynomolgus monkey plasma, we instead employed FXIa as a trigger. Beforehand, we had confirmed, in human FVIII-deficient plasma, that the two triggering conditions produced similar peak heights for the purpose of comparing ACE910 with rhFVIII (Figs 1C and S1). ACE910 improved the peak height of the FXIa-triggered TG assay in FVIII-neutralized cynomolgus monkey plasma in a similar concentration-dependent manner to that in human FVIII-deficient plasma (Fig. 1C,D). ACE910 had a similar cofactor activity as rhFVIII or rpoFVIII in improving the peak height in each species. Beforehand, the rpoFVIII that we prepared had been analyzed for qualification (Fig. S2).

In vivo hemostatic study in an acquired hemophilia A model

To examine the *in vivo* hemostatic potency of ACE910, including that against ongoing bleeds, we modified the non-human primate model of acquired hemophilia A that we previously reported [8]. Briefly, more intense injury procedures were employed, and the dose timing of the test item was set to after the emergence of bleeding symptoms, so that the hemostatic action of 10 U kg^{-1} rpoFVIII could be properly evaluated.